AD_____

Award Number: DAMD17-99-1-9422

TITLE: **The Role of Mitotic Events in Taxol Mediated Apoptosis in Breast Cancer Cells**

PRINCIPAL INVESTIGATOR: **Jennifer A. Pietenpol, Ph.D.**

CONTRACTING ORGANIZATION: Vanderbilt University Medical Center
Nashville, Tennessee 37232-2103

REPORT DATE: December 2000

TYPE OF REPORT: Annual

PREPARED FOR: U.S. Army Medical Research and Materiel Command
Fort Detrick, Maryland 21702-5012

REPORT DOCUMENTATION PAGE

Form Approved
OMB No. 074-0188

1. AGENCY USE ONLY (Leave blank)	2. REPORT DATE	3. REPORT TYPE AND DATES COVERED
	December 2000	Annual (1 Dec 99 - 30 Nov 00)

4. TITLE AND SUBTITLE
The Role of Mitotic Events in Taxol Mediated Apoptosis in Breast Cancer Cells

5. FUNDING NUMBERS
DAMD17-99-1-9422

6. AUTHOR(S)
Jennifer A. Pietenpol, Ph.D.

7. PERFORMING ORGANIZATION NAME(S) AND ADDRESS(ES)
Vanderbilt University Medical Center
Nashville, Tennessee 37232-2103

E-MAIL:
jennifer.pietenpol@mcmail.vanderbilt.edu

8. PERFORMING ORGANIZATION REPORT NUMBER

9. SPONSORING / MONITORING AGENCY NAME(S) AND ADDRESS(ES)
U.S. Army Medical Research and Materiel Command
Fort Detrick, Maryland 21702-5012

10. SPONSORING / MONITORING AGENCY REPORT NUMBER

11. SUPPLEMENTARY NOTES
This report contains colored photos

12a. DISTRIBUTION / AVAILABILITY STATEMENT
Approved for public release; distribution unlimited

12b. DISTRIBUTION CODE

13. ABSTRACT ***(Maximum 200 Words)***

For a drug that is used so widely in breast cancer therapy, little is known about the mechanism of Taxol action. Although Taxol's binding to tubulin is well characterized and the ability of the drug to induce a mitotic arrest is recognized, the biochemical mechanisms by which these events lead to breast cancer cell cytotoxicity are not known. The objective of this research is to test the hypothesis that prolonged activation of Cdc2 and subsequent phosphorylation of Bcl2 are required for Taxol-mediated apoptosis in breast cancer cells. The ultimate goal of the research is to identify a signaling cascade(s) that is important for the cytotoxic effects of Taxol. Progress to date includes: (i) development of cell model systems to analyze the role of Bcl2 phosphorylation in susceptibility to Taxol-mediated apoptosis; (ii) determining that Bcl2 overexpression provides a selective advantage for cell survival and growth in anchorage-independent settings *in vitro* and *in vivo*; and (iii) preliminary confirmation that Taxol-induced modulation of mitotic events that is observed in cell culture models is operational *in vivo*. It is critical to understand how Taxol works at the molecular level in order to pursue rational design of new drugs for the treatment of breast cancer.

14. SUBJECT TERMS
Breast Cancer, Taxol, mitosis, cell cycle

15. NUMBER OF PAGES
25

16. PRICE CODE

17. SECURITY CLASSIFICATION OF REPORT	18. SECURITY CLASSIFICATION OF THIS PAGE	19. SECURITY CLASSIFICATION OF ABSTRACT	20. LIMITATION OF ABSTRACT
Unclassified	Unclassified	Unclassified	Unlimited

NSN 7540-01-280-5500

Standard Form 298 (Rev. 2-89)
Prescribed by ANSI Std. Z39-18
298-102

Table of Contents

INTRODUCTION

For a drug that is used so widely in breast cancer therapy, remarkably little is known about the mechanism of Taxol action. Although Taxol's binding to tubulin is well characterized and the ability of the drug to induce a mitotic arrest is recognized, the biochemical mechanisms by which these events lead to breast cancer cell cytotoxicity after drug administration are not known. A number of cellular signalling pathways have been associated with Taxol's antitumor effects; however, there is a lack of studies that have focused on the role of biochemical pathways activated by Taxol treatment during mitosis, the phase of the cell cycle in which Taxol-treated cells arrest. Knowledge of mitotic signalling pathways that are altered after Taxol treatment of breast cancer cells is critical for our understanding of the drug's mechanism of antitumor action and is the focus of the proposed research. Studies from our laboratory indicate that the anti-apoptotic Bcl2 protein is normally phosphorylated during mitosis and that Taxol treatment of breast cancer cells leads to prolonged mitotic arrest, superphysiologic levels of mitotic kinase activity, and subsequent hyperphosphorylation of Bcl2. Following these events, apoptosis is initiated. Thus, our results provide a link between Taxol-induced elevation of mitotic kinase activity and the apoptotic machinery in the cell. We predict that mitotic cyclin B1/Cdc2 activity is integral for Taxol's cytotoxic activity even though we have found that it is not the kinase directly responsible for mitotic phosphorylation of Bcl2. ***We hypothesize that prolonged activation of Cdc2 and subsequent phosphorylation of Bcl2 are required for Taxol-mediated apoptosis in breast cancer cells.*** We are testing this hypothesis through the specific aims listed below. The ultimate goal of these aims is to identify a signaling cascade that is important for the cytotoxic effects of Taxol and determine if this signalling cascade is operational *in vivo* in breast carcinomas treated with Taxol.

- **Specific Aim 1:** To determine whether Cdc2 activity and Bcl2 phosphorylation are required for Taxol-mediated apoptosis.
- **Specific Aim 2:** To identify the mitotic kinase(s) that phosphorylates Bcl2 in Taxol-treated breast cancer cells
- **Specific Aim 3:** To determine if the Taxol-induced modulation of mitotic events that are observed in cell culture models is operational *in vivo* in xenograft tumors established from breast cancer cell lines

Understanding the link between Taxol modulation of microtubule dynamics, mitotic block, and cell death promises to lead to improved clinical use of the drug in the treatment of breast cancer. It is critical to understand how Taxol works at the molecular level in order to pursue rational design of new drugs for breast cancer that act through alteration of mitotic signalling pathways.

BODY

A description of the research accomplishments associated with each Task outlined in the approved Statement of Work is provided below.

Statement of Work

Task 1: **To determine whether Cdc2 activity and Bcl2 phosphorylation are required for Taxol-mediated apoptosis (months 1-12)**

•Using flow cytometric, cell biology, and protein biochemistry techniques, we will determine the kinetics of mitotic entry and metaphase transition in FT210 cells and if Cdc2 is required for Taxol-mediated apoptosis once cells have entered mitosis (months 1-6)

To address the issue of Cdc2 necessity in Taxol-mediated apoptosis, we have taken advantage of the murine mammary carcinoma cell line, FT210, that contains a temperature-sensitive Cdc2 allele (9). As compared to the parental cell line, FM3A (with wild-type Cdc2), when FT210 cells are grown at the restrictive temperature of 39°C, Cdc2 activity is reduced by >90%, as a result of

rapid degradation of the protein (9). At 32°C, Cdc2 activity is normal in the FT210 cells and the cells rapidly divide. In preliminary experiments, we were able to obtain a G2 arrest (Fig. 1A) accompanied by ~95% loss of cyclinB1/Cdc2 activity after 24 h growth of FT210 cells at the restrictive temperature of 39°C (Fig. 1B). Also, ~95% of FT210 and FM3A cells underwent mitotic arrest after 24 h of Taxol treatment at 32°C (Fig. 1A).

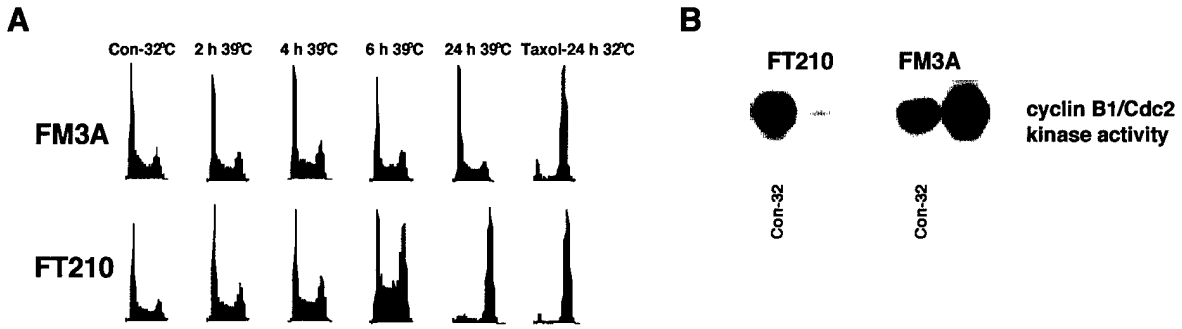

Figure 1. Analysis of FT210 and FM3A cell lines for cell cycle arrest and Cdc2 activity. FM3A and FT210 cells were shifted to 39°C (restrictive temperature for Cdc2 expression—protein is degraded in FT210 cells) for the indicated times and cell harvested for flow cytometric analysis (**A**) or cyclin B1/Cdc2 kinase activity analysis using histone H1 as a substrate (**B**). The cells were also treated with Taxol at 32°C (permissive temperature for Cdc2 activity—protein stable) and cells harvested for flow cytometric analysis.

The FT210 and control FM3A cell lines express murine Bcl2, however, we are also trying to establish FT210 and FM3A cell lines that ectopically express human Bcl2 for the following reasons. First, we would like to confirm all our results with both murine and human Bcl-2 protein. Second, we have found that phosphorylation of murine Bcl2 is not readily detectable using Western analysis and detection requires analyzing protein isolated for $^{32}P_i$-metabolically labeled cells. Thus, analysis will be facilitated by having parallel cell lines containing human Bcl2.

Our intent is to isolate mitotic FT210 cells and derivative human Bcl2-expressing cells by either synchronization methods described below. We will determine the timing of cell entry into mitosis by assessing the onset of cyclin B1/Cdc2 activity, MPM2 positivity and morphology of nuclear and chromosome structure. Once cells have reached prophase, we will shift the cells to the restrictive temperature of 39°C and begin harvested cells at set time intervals and evaluate (a) Cdc2 protein levels, (b) cyclin B1/Cdc2 activity, (c) MPM2 (Mitotic Phosphoprotein Monoclonal-2) positivity, (d) mitotic progression by DAPI-staining, (e) and Bcl-2 isoforms. The FM3A cells will be used as a control in all assays.

Of note, after the first 3 months of work with the FT210 cell line, we determined that it did not represent a clonal population, in other words, it had a mixture of more than one cell type. The heterogeneity in the cell line made it difficult to draw conclusions from the experiments that we had designed, as well as halted our efforts to generate FT210 cells that overexpress human Bcl2. After spending several months trying to obtain the cell line again from the original source as well as other laboratories, we have taken on the task of making clonal populations again, which we are completing at this time. Our intent is to proceed with our original experiments outlined in the proposal once we establish clonal populations. The possibility exists that the cell line is inherently unstable and we may not be able to obtain a clonal population in which Cdc2 activity is under strict control.

After we obtain clonal populations again, the cells will be synchronized by standard technologies in the laboratory, either mimosine treatment which arrests cells at late G1/S or centrifugal elutriation (4,6). Synchronized G1/S cells will be released from mimosine arrest (through drug wash-out) or pure G1 populations of elutriated cells will be placed back in culture. Control or Taxol-treated cells will be allowed to progress through S and G2 phases and into prophase of mitosis. We will determine the window of time in which cells enter mitosis by assessing the onset of cyclin B1/Cdc2 activity, MPM2 positivity and morphology of nuclear and chromosome structure. A previous study by Davis et al. (1) showed that the MPM2 antibody recognizes phosphorylated polypeptides found only in mitotic cells, thus this antibody is a useful reagent for distinguishing 4N

DNA-containing mitotic cells from those in G2-phase by Western, flow cytometric or immunohistochemical analyses. Incubation of cells with Hoescht stain or any other type of DNA stain allows visualization of chromatin condensation, nuclear breakdown, alignment of chromosomes at a metaphase plate, separation of chromosomes at anaphase, and subsequent telophase. Once cells have reached prophase, we will shift the cells to the restrictive temperature of 39°C and begin harvesting cells at set time intervals and evaluate (a) Cdc2 protein levels, (b) cyclin B1/Cdc2 activity, (c) MPM-2 positivity, (d) mitotic progression by Hoescht staining, (e) and apoptotic index by quantification of caspase activation.

•Using molecular biology, cell biology, and protein biochemistry techniques, we will overexpress nonphosphorylatable Bcl2 protein in breast cancer cells and determine the effect protein expression has on mitotic events and susceptibility to Taxol mediated apoptosis (months 6-12)

We have made significant progress on this part of Task 1. We have generated numerous isogenic cell lines that overexpress either pCEP4 (empty episomal mammalian expression vector - Vector control cell lines), pCEP4-Bcl2 (the pCEP4 vector expressing wild-type human Bcl2) or pCEP4-S70 (the pCEP4 vector expressing a mutant S70A-Bcl2 with a substitution mutation at amino acid 70; the serine has been replaced with an alanine - an amino acid that can not be phosphorylated). To date, we have created isogenic sets of the following cell lines: RKO, HCT116, MDA-MB468, and MDA-MB231. We have several clones of each cell line that express significant levels of ectopic Bcl2 protein, either wild-type or mutant. To determine the effect that overexpression of phosphorylatable or nonphosphorylatable Bcl2 has on susceptibility of epithelial tumor cells to Taxol-mediated growth arrest/apoptosis, the isogenic cell lines were assayed for growth in two anchorage-independent systems: soft agar and xenograft tumor. Initially, our analyses were performed on cells grown in the continual presence of Taxol, in the case of the soft agar colonies (Fig. 2), or on cells exposed daily to Taxol (5 of 7 days for three cycles), in the case of the xenograft tumor experiments in athymic nude mice (Fig. 3). Our results from the first set of experiments demonstrated that overexpression of the Bcl-2 (wild-type or the Ser70 mutant form) did not provide significant resistance to continuous Taxol exposure (representative experiments from the RKO cells are shown, Figs. 2 and 3).

Based on the initial results, we set-up a variation of this experiment, in which the cells were exposed to Taxol for 16 h, washed and then placed into soft agar for colony formation or implanted in athymic nude mice and tumor establishment and growth assessed. Our rationale for this second approach was to parallel what happens clinically in the treatment of breast tumors. It is predicted that after Taxol infusion, the patient has circulating Taxol at ~75 nM for 18-24 h after which time it is cleared (personal communication, David Johnson, M.D., Vanderbilt Ingram Cancer Center). Thus, we tried to recapitulate this scenario with a 16 h transient exposure of cells to Taxol followed by a washout and transfer to an anchorage-independent medium to allow assessment of survival and proliferation.

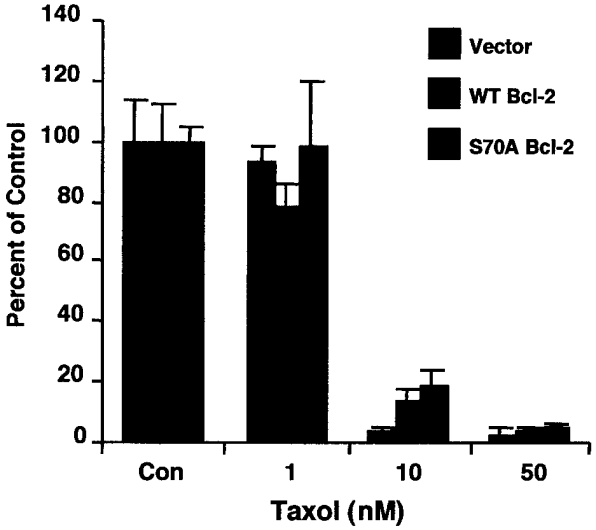

Figure 2. Achorage independent growth of RKO cell lines overexpressing Bcl2. RKO-Vector, RKO-Bcl2, and RKO-S70A-Bcl2 cells were plated at 1 x 10^4 per 35 mm dish in McCoy's 5A medium supplemented with 10% fetal bovine serum, 0.4% agar, and the indicated concentrations of Taxol. Colonies were counted after 7 days using an Omnicon FACS III image analyzer (Bausch & Lomb). Values are representative of two independent experiments carried out in triplicate. Data are plotted as percent of control.

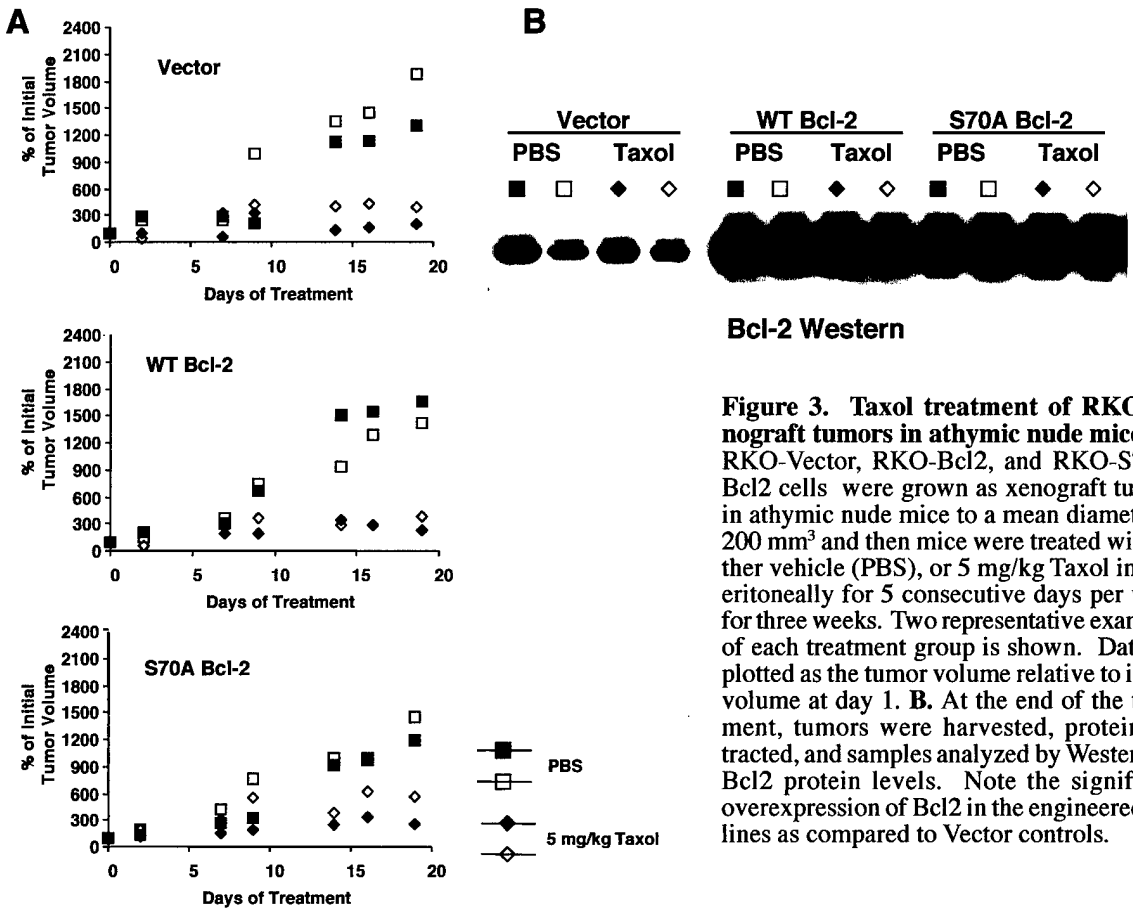

Figure 3. Taxol treatment of RKO xenograft tumors in athymic nude mice. A. RKO-Vector, RKO-Bcl2, and RKO-S70A-Bcl2 cells were grown as xenograft tumors in athymic nude mice to a mean diameter of 200 mm^3 and then mice were treated with either vehicle (PBS), or 5 mg/kg Taxol intraperitoneally for 5 consecutive days per week for three weeks. Two representative examples of each treatment group is shown. Data are plotted as the tumor volume relative to initial volume at day 1. **B.** At the end of the treatment, tumors were harvested, protein extracted, and samples analyzed by Western for Bcl2 protein levels. Note the significant overexpression of Bcl2 in the engineered cell lines as compared to Vector controls.

In particular, we were interested in determining if Bcl2 overexpression allowed a selective survival and growth advantage to tumor cells growing in an anchorage-independent fashion. The results of these experiments are shown in Figure 4 (soft agar results) and Figure 5 (xenograft tumor results). In summary, overexpression of wild-type Bcl2, but not the Ser70 mutant form of Bcl2 conferred a survival advantage to tumor cells after a transient 16 h exposure to Taxol and allowed establishment and growth of tumor cells in an anchorage-independent manner. These results are currently being prepared for publication.

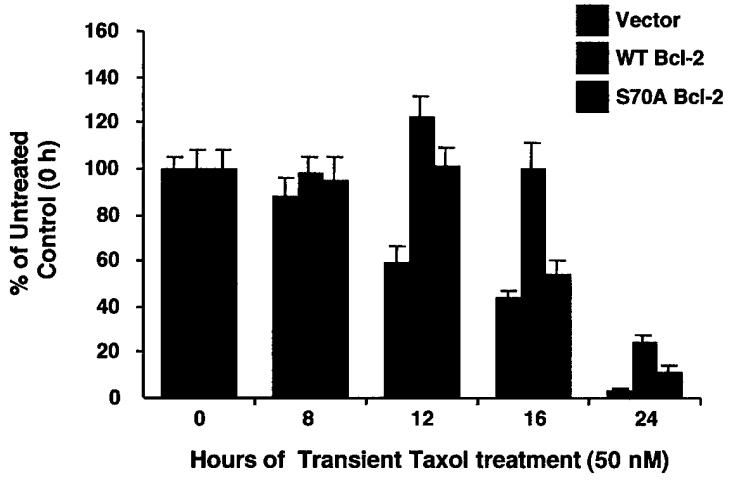

Figure 4. Achorage independent growth of RKO cell lines transient exposure to Taxol. RKO-Vector, RKO-Bcl2, and RKO-S70A-Bcl2 cells were exposed to 50 nM Taxol for the indicated times after which the cells were washed and plated at 1 x 10^4 per 35 mm dish in McCoy's 5A medium supplemented with 10% fetal bovine serum, 0.4% agar, and the indicated concentration of Taxol. Colonies were counted after 7 days using an Omnicon FACS III image analyzer (Bausch & Lomb). Values are representative of two independent experiments carried out in triplicate. Data are plotted as percent of control.

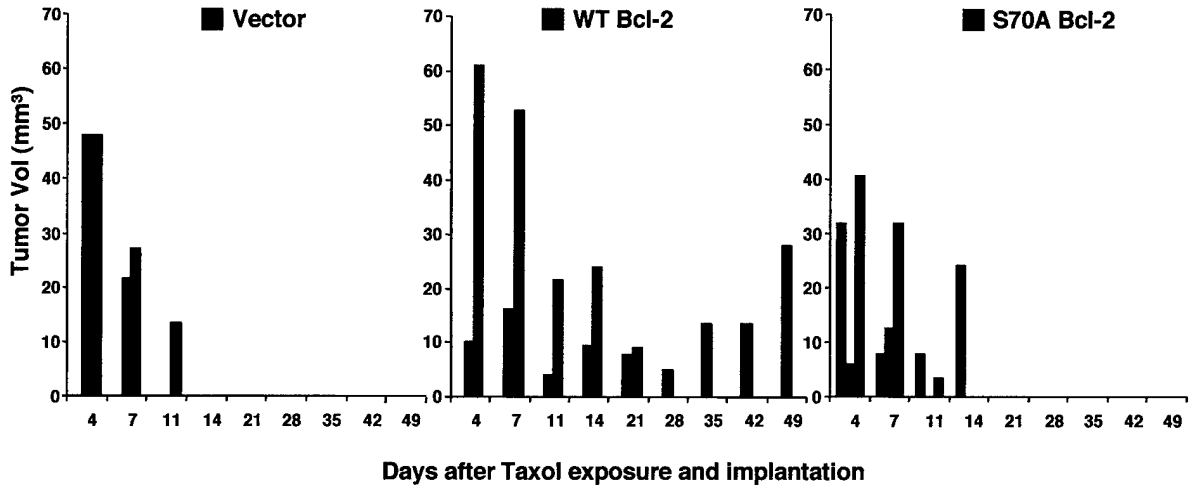

Figure 5. Ability of RKO cell lines to form xenograft tumors after transient exposure to Taxol. RKO-Vector, RKO-Bcl2, and RKO-S70A cells were exposed to 50 nM Taxol for 16 h, washed, and injected into athymic nude mice. Xenograft tumor formation and growth were followed by weekly measurements which are plotted as acutal tumor volume Note the persistance of the Bcl2-expressing tumors.

•Taxol-mediated phosphorylation of p53 in epithelial tumor cells

From related studies in the laboratory and preliminary results obtained from several experiments in the first year of this grant, we also deduced that the status of p53 checkpoint function in breast tumor cells was an important determinant for Taxol-induced apoptosis. Since p53 directly regulates the cyclin-dependent kinase inhibitor p21 (2) that can inhibit cyclin B1/Cdc2 activity in the cell and thus G2/M transition (3), the p53 protein can also indirectly regulate Bcl2 phosphorylation. Our results demonstrate that after Taxol treatment, epithelial tumor cells arrest in mitosis and either undergo apoptosis or aberrantly exit mitosis and enter G1 with a 4N DNA content (7,8). When the latter event occurs in tumor cells with defective G1/S checkpoint function, due to loss of proteins such as p53 or its downstream target p21, the cells enter into S-phase with a 4N DNA content and become polyploid, a process known as endoreduplication. Once a cell undergoes aberrant mitotic slippage and endoreduplication, we have found that it has enhanced chemosensitivity to Taxol in both *in vitro* and *in vivo* tumor models (8). These studies, that identified a role for p53 signaling in Taxol chemosensitivity led us to examine the upstream signaling pathway(s) that activate p53 after mitotic slippage in epithelial tumor cells, in particular if Taxol induces phosphorylation of p53 and, if so, on what residues and how this compares to that induced by other anti-cancer agents. This work is directly relevant to this grant since p53 mutation is one of the most frequent alterations in breast tumors and Taxol is a leading chemotherapeutic agent for treatment of breast cancer. Thus, any information we obtain about the role of p53 signaling in Taxol chemosensitivity from our cell and animal model systems (that we are using for Bcl2 analyses) will have important implications for both clinical treatment of breast cancer and identification of molecular targets for chemotherapeutic intervention. The results of our recent study are presented in a paper that will be published in *Oncogene*, January 2001 (see Appendix).

Task 2: **To identify the mitotic kinase(s) that phosphorylates Bcl2 in Taxol-treated breast cancer cells (months 13-36)**

•Large scale protein preparation and column chromatography will be performed accompanied by enzyme activity assays (months 1-24)
•Peptide sequencing of purified protein(s), cDNA cloning, and further characterization of gene and protein will be performed (e.g. initiate antibody production, analyze cell cycle regulation of candidate kinase) (months 24-36)

To date we have constructed the recombinant Bcl2 expression vectors and begun Bcl2 protein scale-up for column preparation. We have found that production of recombinant Bcl2 in *E. Coli* gives a very low yield due to the fact that most of the protein is present in occlusion bodies. Currently, we are contemplating switching to a baculovirus expression system. Nonetheless, we have produced enough Bcl2 to begin small-scale testing of protein extracts from Taxol-treated MDA-MB468 cells. In the grant we also proposed to use FT210 cells since they grow in suspension to high density and therefore the cost of large scale expansion would be relatively moderate. However, for the reasons discussed above, we are refraining from using the FT210 cells until we clarify the clonality issue. To date, we have made small glutathione resin columns that have GST-Bcl2 attached. After column preparation, we introduced protein extracts from control or Taxol-treated MDA-MB468 cells onto the column, washed with physiological buffer conditions, eluted supposed Bcl2-bound proteins with a high salt, and examined the profile of proteins (by PAGE followed by silver staining) that were bound to the Bcl2. Our findings after our first trials, suggest that the protein profiles are different from control extracts as compared to those from Taxol-treated cells. We will likely turn to mass spectrometry for mass determination as well as peptide sequencing for identification of the proteins that are bound to the recombinant Bcl2. Of note, all protein extracts were first passed over a control glutathione column that only contains GST so that proteins that bind non-specifically to glutathione or GST are excluded from our analyses. Our plans for the coming year of the grant include scaling up our protein production as well as use of mass spectrometry for more of the analyses to minimize the amount of protein required.

***Task 3:* To determine if the Taxol-induced modulation of mitotic events that are observed in cell culture models is operational *in vivo* in xenograft tumors established from breast cancer cell lines (months 136).**

•Initiate breast cancer cell line xenograft tumors in nude mice (month 1)
•Taxol treatment and analysis of tumor volume as well as flow cytometric analysis of tumors (month 2)
•Immunohistochemical and protein biochemical analysis of tumor samples (month 3-6)
oat least 3 reiterative cycles of the above anticipated over the 1-36 month time period

Xenograft tumors were established from MDA-MB468, RKO, and MDA-MB231 breast carcinoma cell lines. We were unable to obtain robust xenograft tumors with MCF-7 cells. Of the cell lines that gave positive results, tumors began to form in 14-21 days. In the first sets of experiments, Taxol was given initially at two doses (10 mg/kg/day and 5 mg/kg/day) for 4 consecutive days and depending on tumor response for another 4-5 day interval. Animals received Taxol or vehicle control (Cremophor) via IP injections and the tumor volume was measured biweekly. At set intervals (every 5 days during the first round of experimentation), tumor biopsies were performed and tissue harvested for: (i) flow cytometric analyses as we have previously performed on murine tumors (5), (ii) protein preparation for Western and Cdc2 kinase assays, and (iii) sectioning and immunohistochemistry to evaluate *in situ* cell cycle analyses with MPM2 antibodies. MPM2 staining patterns allowed us to determine the percentage of cells present in mitosis at any given time in control and taxol-treated tumor biopsies. To date we have been able to establish tumors with the cell lines indicated above as well as the isogenic sets of cell lines that express either vector alone, wild-type or the phospho-mutant Bcl2 as described in Task 1. Furthermore, we have performed preliminary experiments with MDA-MB231 xenograft tumors that formed in athymic nude mice and analyzed tumor biopsies from control and Taxol-treated animals for MPM2 positivity by immunohistochemistry (Fig. 6A) or for cell cycle protein levels and activity (Fig. 6B). Note the high level of MPM2 immunopositivity (pink-stained nuclei) in the xenograft tumor section from Taxol-treated animals. The MPM2 positivity in (Fig. 6A) correlates with the MPM2 signal observed by Western analysis in (Fig. 6B). Moreover, the MPM2 positivity which is indicative of mitotic cells correlates well with two other markers of mitosis: phosphorylated Bcl-2 and elevated levels of cyclinB-associated kinase activity. The cyclin B protein levels are relatively the same between samples since cyclin B1 is expressed in rapidly proliferating cells in S, G2, and M- phases.

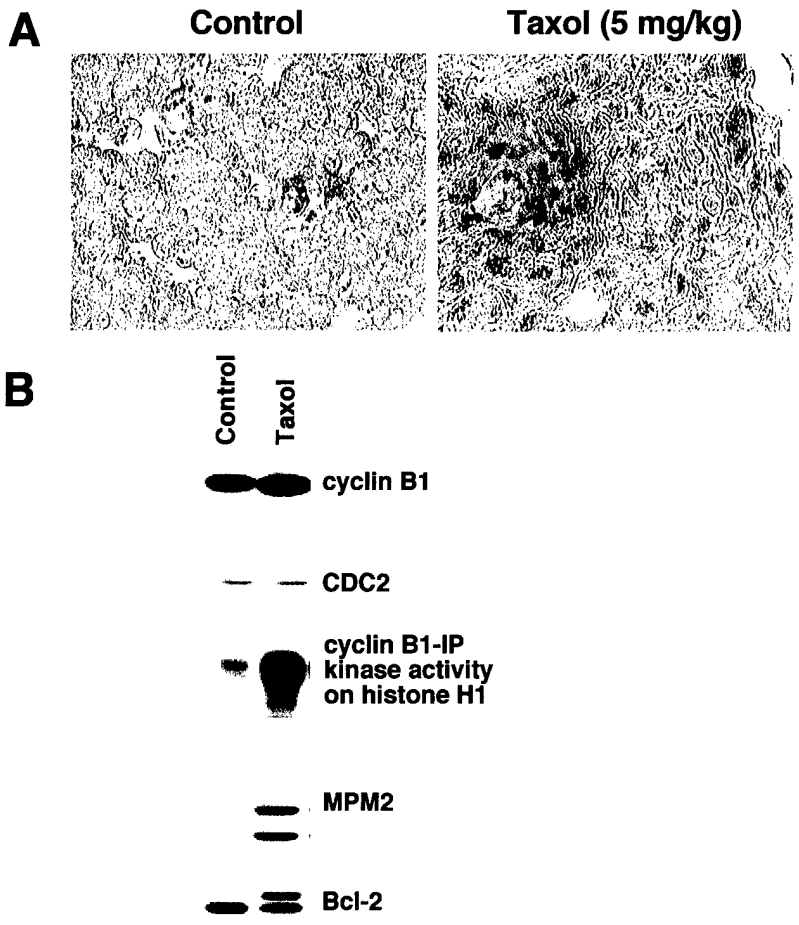

Figure 6. Taxol treatment of MDA-MB231 xenograft tumors in athymic nude mice. MDA-MB231 cells (5 x 10^6) were resuspended in 0.2 ml of media and injected subcutaneously into the flanks of female 4-6 week old athymic nude mice (Harlan Sprague Dawley). The resulting xenograft tumors were allowed to grow to a mean size of 200 mm^3. Mice with a similar range in tumor sizes were treated with either vehicle (PBS)- Control, or 5 mg/kg Taxol (Meade-Johnson) intraperitoneally for 2 consecutive days. Tumors were harvested, parrafin embedded and processed for immunohostochemistry with anti-MPM2 antibodies (A) or lysates were prepared for Western and kinase assays (B).

KEY RESEARCH ACCOMPLISHMENTS

•Development of isogenic cell model systems to analyze the effect of wild-type or phospho-mutant Bcl2 expression on mitotic events and susceptibility to Taxol-mediated apoptosis.

•Determination that after a transient exposure of epithelial tumor cells to Taxol, Bcl2 overexpression provides a selective advantage for cell survival and growth in anchorage-independent settings *in vitro* and *in vivo*.

•Preliminary confirmation that the Taxol-induced modulation of mitotic events that is observed in cell culture models is operational *in vivo* in xenograft tumors established from breast cancer cell lines.

REPORTABLE OUTCOMES

•Stewart, Z.A., Tang, L.J., and Pietenpol, J.A. (2001) Increased p53 phosphorylation after microtubule disruption is mediated in a microtubule inhibitor- and cell-specific manner. *Oncogene* In Press, January.

CONCLUSIONS

The main objective of this research is to test the hypothesis that prolonged activation of Cdc2 and subsequent phosphorylation of Bcl2 are required for Taxol-mediated apoptosis in breast cancer cells. The ultimate goal of our research is to identify a signaling cascade that is important for the cytotoxic effects of Taxol and determine if this signaling cascade is operational *in vivo* in breast carcinomas treated with Taxol. Our progress described above continues to forge the the link between Taxol modulation of microtubule dynamics, mitotic block, and cell death and promises to lead to improved clinical use of the drug in the treatment of breast cancer. It is critical to understand how Taxol works at the molecular level in order to pursue rational design of new drugs for the treatment of breast cancer that act through alteration of mitotic signaling pathways.

Furthermore, these studies continue to represent a novel area of investigation — exploring cell cycle changes *in vitro* and *in vivo* after Taxol treatment of breast cancer tumor cells. In fact, the data from the first year of funding provided the necessary preliminary data to proceed with similar studies using tumor material from patients enrolled in a Taxol-based clinical trial at the Vanderbilt-Ingram Cancer Center (these related studies are funded by a Discovery grant from the Vanderbilt-Ingram Cancer Center).

REFERENCES

1. **Davis, F. M., T. Y. Tsao, S. K. Fowler, and P. N. Rao.** 1983. Monoclonal antibodies to mitotic cells. Proc. Natl. Acad. Sci. U. S. A. **80**:2926-2930.

2. **El-Deiry, W. S., T. Tokino, V. E. Velculescu, D. B. Levy, R. Parsons, J. M. Trent, D. Lin, W. E. Mercer, K. W. Kinzler, and B. Vogelstein.** 1993. *WAF1*, a potential mediator of p53 tumor suppression. Cell **75**:817-825.

3. **Flatt, P. M., L. J. Tang, C. D. Scatena, S. T. Szak, and J. A. Pietenpol.** 2000. p53 Regulation of G_2 checkpoint is retinoblastoma protein dependent. Mol. Cell. Biol. **20**:4210-4223.

4. **Leach, S. D., C. D. Scatena, C. J. Keefer, H. A. Goodman, S. Y. Song, L. Yang, and J. A. Pietenpol.** 1998. Negative regulation of Wee1 expression and Cdc2 phosphorylation during p53-mediated growth arrest and apoptosis. Cancer Res. **58**:3231-3236.

5. **Norgaard, P., B. Law, H. Joseph, D. L. Page, Y. Shyr, D. Mays, J. A. Pietenpol, N. E. Kohl, A. Olliff, R. J. Coffey Jr, H. S. Poulsen, and H. L. Moses.** 1998. Treatment with farnesyl-protein transferase inhibitor induces regression of mammary tumors in TGFα and TGFα/*neu* transgenic mice by inhibition of mitogenic activity and induction of apoptosis. Proc. Natl. Acad. Sci. U. S. A. **In press**:

6. **Scatena, C. D., Z. A. Stewart, D. Mays, L. Tang, C. Keefer, S. D. Leach, and J. A. Pietenpol.** 1998. Mitotic phosphorylation of Bcl-2 during normal cell cycle progression and Taxol-induced growth arrest. J. Biol. Chem. **13**:30777-30784.

7. **Stewart, Z. A., S. D. Leach, and J. A. Pietenpol.** 1999. $p21^{Waf1/Cip1}$ inhibition of cyclin E/Cdk2 activity prevents endoreduplication after mitotic spindle disruption. Mol. Cell. Biol. **19**:205-215.

8. **Stewart, Z. A., D. Mays, and J. A. Pietenpol.** 1999. Defective G_1-S cell cycle checkpoint function sensitizes cells to microtubule inhibitor-induced apoptosis. Cancer Res. **59**:3831-3837.

9. **Th'ng, J. P. H., P. S. Wright, J. Hamaguchi, M. G. Lee, C. J. Norbury, P. Nurse, and E. M. Bradbury.** 1990. The FT210 cell line is a mouse G2 phase mutant with a temperature-sensitive *CDC2* gene product. Cell **63**:313-324.

APPENDIX

Contents: 1 journal article

•Stewart, Z.A., Tang, L.J., and Pietenpol, J.A. (2001) Increased p53 phosphorylation after microtubule disruption is mediated in a microtubule inhibitor- and cell-specific manner. *Oncogene* In Press, January.

Galley proof

Oncogene (2001) 00, 00–00

www.nature.com/onc

Increased p53 phosphorylation after microtubule disruption is mediated in a microtubule inhibitor- and cell-specific manner

Zoe A Stewart[1], Luo Jia Tang[1] and Jennifer A Pietenpol*,[1]

[1]*Department of Biochemistry, Center in Molecular Toxicology, and the Vanderbilt-Ingram Cancer Center, Vanderbilt University School of Medicine, Nashville, Tennessee TN 37232, USA*

p53 is present at low levels in unstressed cells. Numerous cellular insults, including DNA damage and microtubule disruption, elevate p53 protein levels. Phosphorylation of p53 is proposed to be important for p53 stabilization and activation after genotoxic stress; however, p53 phosphorylation after microtubule disruption has not been analysed. The goal of the current study was to determine if p53 phosphorylation increases after microtubule disruption, and if so, to identify specific p53 residues necessary for microtubule inhibitor-induced phosphorylation. Two dimensional gel analyses demonstrated that the number of p53 phospho-forms in cells increased after treatment with microtubule inhibitors (MTIs) and that the pattern of p53 phosphorylation was distinct from that observed after DNA damage. p53 phosphorylation also varied in a MTI-dependent manner, as Taxol and Vincristine induced more p53 phospho-forms than nocodazole. Further, MTI treatment increased phosphorylation of p53 on serine-15 in epithelial tumor cells. In contrast, serine-15 phosphorylation of p53 did not increase in MTI-treated primary cultures of human fibroblasts. Analysis of ectopically expressed p53 phospho-mutant proteins from Taxol- and nocodazole-treated cells indicated that multiple p53 amino terminal residues, including serine-15 and threonine-18, were required for Taxol-mediated phosphorylation of p53. Taken together, the results of this study demonstrate that distinct p53 phospho-forms are induced by MTI treatment as compared to DNA damage and that p53 phosphorylation is mediated in a MTI- and cell-specific manner. *Oncogene* (2001) **20**, 000–000.

Keywords: taxol; vincristine; nocodazole; adriamycin; ionizing radiation; ATM; DNA damage.

Introduction

The p53 tumor suppressor protein is present at low levels in unstressed cells, likely due to MDM2 binding and targeting p53 for ubiquitin-mediated degradation (Kubbutat *et al.*, 1997; Haupt *et al.*, 1997). However, cellular insults, such as DNA damage, oncogenic stimuli, or microtubule disruption, elevate p53 protein levels. While upstream p53 signaling pathways induced by genotoxic stress and oncogenic stimuli have been identified, pathways that mediate p53 activation after microtubule disruption have not been elucidated. Cells lacking p53-dependent signaling undergo endoreduplication and become polyploid after microtubule inhibitor (MTI) treatment (Cross *et al.*, 1995; Di Leonardo *et al.*, 1997; Khan and Wahl, 1998; Lanni and Jacks, 1998; Stewart *et al.*, 1999a). Further, tumor cells with defective p53-mediated G1/S checkpoint function are sensitized to MTI treatment *in vivo* (Stewart *et al.*, 1999b). Since drugs that alter microtubule dynamics are widely used chemotherapeutic agents, identifying the signaling pathways involved in p53 activation after microtubule disruption may have important therapeutic implications.

After genotoxic stress, phosphorylation of p53 may be important for p53 stabilization. Numerous cellular kinases mediate phosphorylation of p53 after ionizing radiation (IR) and ultraviolet radiation (UV). Several members of the phosphoinositide-3 kinase (PI-3K) family can directly phosphorylate p53 on amino terminal residues after both IR and UV treatment, including DNA-activated protein kinase (DNA-PK), ataxia-telangiectasia mutated (ATM) kinase and ATM-related kinase (ATR) (Lees-Miller *et al.*, 1992; Canman *et al.*, 1998; Banin *et al.*, 1998; Tibbetts *et al.*, 1999; Hall-Jackson *et al.*, 1999). DNA-PK is activated by DNA double-strand breaks and phosphorylates p53 on Ser-15 and Ser-37 *in vitro* (Lees-Miller *et al.*, 1992). ATM is also activated by DNA double-strand breaks and phosphorylates p53 on Ser-15 *in vitro* (Canman and Lim, 1998; Canman *et al.*, 1998). ATM function is defective in patients with ataxia-telangiectasia (AT), a disorder in which patients have increased sensitivity to radiation and are highly cancer prone (Lavin and Shiloh, 1996). Cells from AT patients have delayed p53 stabilization and significantly diminished Ser-15 phosphorylation after IR exposure (Siliciano *et al.*, 1997; Shieh *et al.*, 1997; Canman *et al.*, 1998). ATR phosphorylates p53 on both Ser-15 and Ser-37 *in vitro* and overexpression of a catalytically inactive ATR reduces Ser-15 phosphorylation at late times after IR (Tibbetts *et al.*, 1999; Hall-Jackson *et al.*, 1999). DNA-PK and ATM also phosphorylate MDM2 after DNA damage, preventing formation of the p53-MDM2 complex (Mayo *et al.*, 1997; Khosravi *et al.*, 1999).

*Correspondence: JA Pietenpol
Received 14 August 2000; revised 16 October 2000; accepted 26 October 2000

Thus, post-translational regulation of the p53-MDM2 interaction likely occurs by modifications on both proteins.

ATM-dependent signaling induced by DNA damage also results in the activation of the Chk1 and Chk2 kinases (Matsuoka *et al.*, 1998; Sanchez *et al.*, 1997; Furnari *et al.*, 1997). Chk1- and Chk2-mediated phosphorylation of p53 on Ser-20 may be important for p53 stabilization after DNA damage (Hirao *et al.*, 2000; Shieh *et al.*, 2000; Chehab *et al.*, 2000). Chk2 phosphorylates p53 on Ser-20 *in vitro* and this phosphorylation dissociates p53-MDM2 complexes (Chehab *et al.*, 2000). Additionally, Chk2−/− embryonic stem cells fail to maintain IR-induced cell cycle arrest, a phenotype similar to that of p53−/− cells (Hirao *et al.*, 2000). Further, wild type (wt) Chk1 phosphorylates p53 on Ser-20 *in vitro* and overexpression of Chk1 increases levels of p53 protein in cells (Shieh *et al.*, 2000). Since mutation of Ser-20 to alanine abrogates p53 stabilization after both IR and UV exposure (Chehab *et al.*, 1999), Chk1 and Chk2 may play an important role in DNA damage-induced p53 activation.

Several other cellular kinases mediate phosphorylation of p53 after genotoxic stress. The p38 stress-activated kinase phosphorylates p53 on Ser-33 and Ser-46 afer UV radiation but not IR (Bulavin *et al.*, 1999). Inhibition of p38 kinase activity or mutation of Ser-33 and Ser-46 to alanines reduced p53-mediated apoptosis and decreased sensitivity to UV radiation, suggesting p38 plays an important role in p53 signaling after UV exposure (Bulavin *et al.*, 1999). Casein kinase I (CKI) phosphorylates murine p53 on Ser-4, Ser-6, and Ser-9 *in vitro* (Milne *et al.*, 1992; Knippschild *et al.*, 1997). CKI also phosphorylates human p53 on Thr-18 *in vitro*, a modification that required prior Ser-15 phosphorylation (Dumaz *et al.*, 1999; Sakaguchi *et al.*, 2000). However, further studies are necessary to determine if CKI phosphorylates p53 on Thr-18 after DNA damage *in vivo*.

Numerous kinases and phosphatases regulate the phosphorylation of p53 on carboxy terminal sites. Both casein kinase II and the double stranded RNA-activated protein kinase PKR phosphorylate p53 on Ser-392, a modification proposed to control p53-mediated transactivation (Hupp *et al.*, 1992; Hall *et al.*, 1996; Cuddihy *et al.*, 1999). Protein kinase C mediates phosphorylation of three carboxy terminal serine residues of p53: Ser-371, Ser-376, and Ser-378 (Baudier *et al.*, 1992). Of note, Ser-376 and Ser-378 are constitutively phosphorylated in cells, and Ser-376 is dephosphorylated in response to DNA damage in an ATM-dependent manner (Waterman *et al.*, 1998). Dephosphorylation of Ser-376 results in enhanced binding of 14-3-3 proteins to p53 and mediates increased sequence-specific DNA binding by p53 (Waterman *et al.*, 1998). Finally, phosphorylation of Ser-315 by Cdk2 and Cdc2, as well as dephosphorylation by Cdc14, may influence the nuclear localization of p53 and regulate p53 binding to a subset of p5t3 consensus DNA binding sites (Wang and Prives, 1995; Hecker *et al.*, 1996; Li *et al.*, 2000).

Several p53 upstream signaling pathways induced by genotoxic stress and oncogenic stimuli (Sherr and Weber, 2000) have been determined in recent years; however, the mechanism(s) by which p53 is activated after microtubule disruption has not been identified. The goal of the current study was to determine if p53 phosphorylation increases after microtubule disruption, and if so, to identify specific p53 residues necessary for MTI-induced phosphorylation. The results demonstrate that distinct p53 phospho-forms are induced by MTI treatment as compared to DNA damage. Phosphorylation of p53 on Ser-15 increased in epithelial tumor cells but not in non-transformed fibroblasts after microtubule disruption. Further, multiple p53 amino terminal residues, including Ser-15 and Thr-18, were required for Taxol-induced phosphorylation of ectopically expressed p53 phospho-mutant proteins.

Results

Taxol and vincristine treatments induce multiple p53 phospho-forms

To analyse p53 phosphorylation after microtubule disruption, protein lysates were prepared from control and Taxol-treated HCT116 cells, and p53 was analysed by two dimensional (2D) gel electrophoresis. Taxol treatment of HCT116 cells resulted in a significant increase in the number and amount of phospho-forms detected by 2D analysis as compared to those observed in a control lysate (Figure 1a). We analysed 1 mg of control lysates as compared to 150 μg of protein lysate from Taxol-treated cells to ensure that the additional p53 phospho-forms observed in the treated samples were a reflection of stress-induced changes and not merely higher p53 protein levels. The faster migrating phospho-form labeled S represents an internal standard provided by the admixture of a recombinant carboxy terminal truncated human p53 protein (amino acids 1–353) (Szak and Pietenpol, 1999) to the IEF sample buffer (Figure 1a). To confirm that the multiple p53 species detected by 2D analysis were a result of phosphorylation, an aliquot of the Taxol-treated HCT116 lysate was incubated with potato acid phosphatase prior to 2D analysis. Phosphatase treatment collapsed the phospho-forms to a single species of protein labeled P_0 (Figure 1a). Sequential phospho-forms are indicated as P_1 and P_2; phospho-forms beyond P_2 were not assigned. Of note, each of the various p53 phospho-forms (P_0, P_1, P_2, etc.) likely comprise a mixture of phosphorylated p53 species with identical mass/charge ratios.

To compare MTI-induced p53 phosphorylation to that induced by genotoxic stress, protein lysates were prepared from HCT116 cells treated with MTIs (Taxol, Vincristine, nocodazole) and DNA damaging agents (IR, ADR, UV) and evaluated by 2D gel electrophoresis. All treatments except nocodazole induced an increase in the relative number of p53 phospho-forms beyond those present in the control lysate, as well as a

distinct p53 phosphorylation pattern (Figure 1b). The different patterns of p53 phospho-forms induced by Taxol, Vincristine, and nocodazole treatments also suggest distinct signaling pathways are activated by these MTIs (Figure 1b).

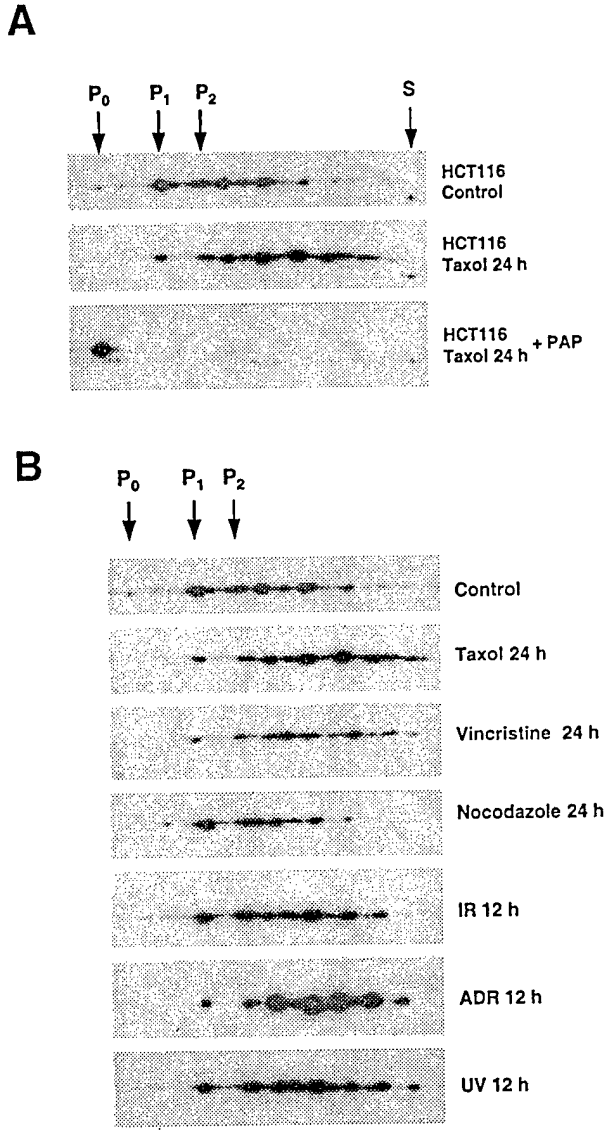

Figure 1 Taxol and Vincristine treatments induce multiple p53 phospho-forms. (a) Lysates from control and Taxol-treated (100 nM) HCT116 cells were analysed by 2D gel electrophoresis. To verify that the p53 forms were a result of phosphorylation, parallel lysates prepared from Taxol-treated cells were treated with potato acid phosphatase (PAP) prior to 2D gel analysis. S denotes the migration of the internal standard protein, a truncated form of human p53. P_0 indicates the migration of unphosphorylated p53, while P_1 and P_2 denote various phospho-forms of p53. The various p53 phospho-forms (P_0, P_1, P_2) likely comprise a mixture of phosphorylated p53 species with identical mass/charge ratios. (b) Lysates from control and cells treated with Taxol (100 nM), Vincristine (100 nM), nocodazole (83 nM), IR (10 Gy), ADR (350 nM), or UV (100 mJ) for the indicated times were analysed by 2D gel electrophoresis. Samples were evaluated with the PAb1801 antibody. Results are representative of three independent experiments

Serine-15 phosphorylation of p53 is increased in MTI-treated tumor cells

After exposure of cells to genotoxic agents, p53 phosphorylation on Ser-15 increases and is proposed to play a role in p53 stabilization (Canman *et al.*, 1998; Banin *et al.*, 1998; Craig *et al.*, 1999). To determine if microtubule disruption induces phosphorylation of p53 on Ser-15, protein lysates from HCT116 cells treated with Taxol and nocodazole were examined by Western analysis using an antibody specific to p53 phosphorylated at Ser-15. Samples were also evaluated to assess total p53 protein levels and changes in the protein levels of the p53 downstream targets MDM2 and p21. For comparison, lysates from IR- and ADR-treated HCT116 cells were also analysed.

After treatment of HCT116 cells with Taxol or nocodazole, an increase in total p53 protein levels was detectable by 12 h (Figure 2a, PAb1801). The increase in p53 after nocodazole treatment was accompanied by elevations in MDM2 and p21 protein levels. In contrast, after Taxol treatment, the elevation in p53 protein was accompanied by a decrease in MDM2 protein levels (Figure 2a). Ser-15 phosphorylation of p53 also increased above control levels in nocodazole- and Taxol-treated cells. Fluoroimager analyses were performed to quantify the PAb1801 and the α-Ser-15 p53 chemiluminescent signals to determine the fold increase of total p53 and Ser-15 phosphorylated p53 relative to control for each treatment; these numbers appear below the PAb1801 and the α-Ser-15 p53 panels in Figure 2a. Treatment with both MTIs increased p53 Ser-15 phosphorylation for all timepoints evaluated (Figure 2a). For example, after 12 h Taxol treatment, there was a 3.6-fold increase in Ser-15 phosphorylated p53 as compared to a 1.6-fold increase in total p53 protein (Figure 2a). After IR and ADR treatments, the levels of total p53 protein and Ser-15 phosphorylated p53 increased for all timepoints examined, consistent with previous studies (Canman *et al.*, 1998; Gao *et al.*, 1999), and was accompanied by elevations in MDM2 and p21 protein levels (Figure 2a).

To verify the results obtained in the HCT116 cells, total p53 and Ser-15 phosphorylated p53 levels were analysed in the RKO human colon carcinoma cell line after treatment (Figure 2b). Similar to HCT116 cells, MTIs and DNA damaging agents induced an elevation in Ser-15 phosphorylated p53 greater than the elevation in total p53 protein for all timepoints (Figure 2b). For example, after 48 h nocodazole treatment, there was a 18.2-fold increase in Ser-15 phosphorylated p53 as compared to a 8.5-fold increase in total p53 protein (Figure 2b). Comparable increases in Ser-15 phosphorylated p53 and total p53 were observed after 48 h Taxol treatment, as the increase in Ser-15 phosphorylated p53 was a fold greater than that observed for total p53 protein levels (Figure 2b). Like the HCT116 cells, the increase in p53 after nocodazole, IR, and ADR treatments was accompanied by elevations in

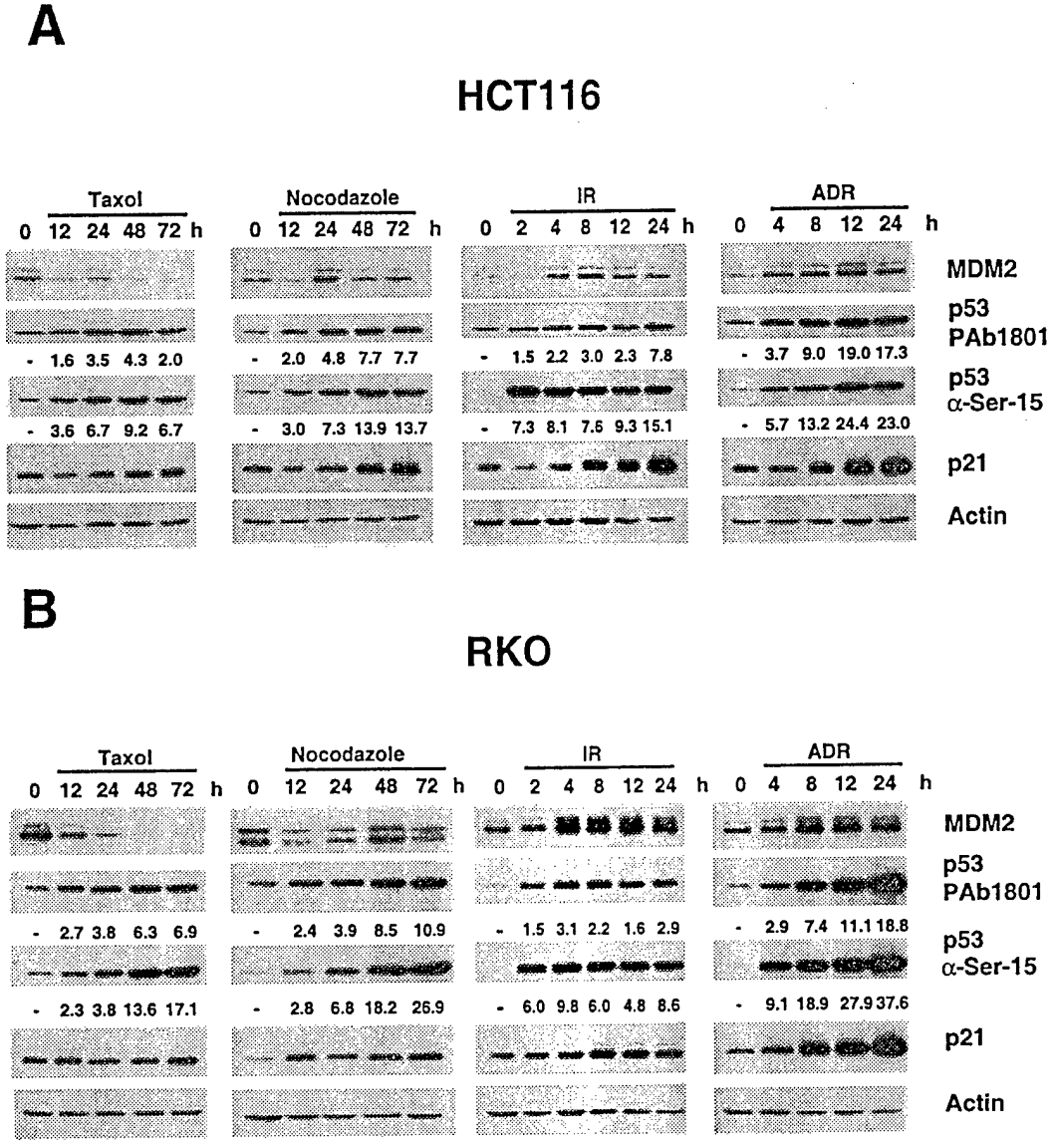
A
HCT116
Taxol
0 12 24 48 72 h
- 1.6 3.5 4.3 2.0
- 3.6 6.7 9.2 6.7
Nocodazole
0 12 24 48 72 h
- 2.0 4.8 7.7 7.7
- 3.0 7.3 13.9 13.7
IR
0 2 4 8 12 24 h
- 1.5 2.2 3.0 2.3 7.8
- 7.3 8.1 7.5 9.3 15.1
ADR
0 4 8 12 24 h
- 3.7 9.0 19.0 17.3
- 5.7 13.2 24.4 23.0
MDM2
p53 PAb1801
p53 α-Ser-15
p21
Actin
B
RKO
Taxol
0 12 24 48 72 h
- 2.7 3.8 6.3 6.9
- 2.3 3.8 13.6 17.1
Nocodazole
0 12 24 48 72 h
- 2.4 3.9 8.5 10.9
- 2.8 6.8 18.2 25.9
IR
0 2 4 8 12 24 h
- 1.5 3.1 2.2 1.6 2.9
- 6.0 9.8 6.0 4.8 8.6
ADR
0 4 8 12 24 h
- 2.9 7.4 11.1 18.8
- 9.1 18.9 27.9 37.6
MDM2
p53 PAb1801
p53 α-Ser-15
p21
Actin
C
NOC TAX
0 24 48 24 48 h
MDM2
- 3.1 2.2 2.7 2.3
p21
- 4.4 5.1 5.8 9.6
GADPH
- 1.1 1.0 1.1 0.9

MDM2 and p21 protein levels, while MDM2 protein levels decreased after Taxol treatment in the RKO cells (Figure 2b).

To determine if the decrease in MDM2 protein levels after Taxol treatment was mediated by transcriptional regulation of the MDM2 promoter, Northern analyses were performed on mRNA isolated from nocodazole- and Taxol-treated HCT116 cells. Both nocodazole and Taxol treatment resulted in increased MDM2 and p21 mRNA levels after 24 and 48 h of treatment (Figure 2c). Thus, the reduction in MDM2 protein levels after Taxol treatment was not a consequence of a decrease in MDM2 mRNA.

Increased serine-15 phosphorylation of p53 after MTI treatment occurs in a cell-specific manner

ATM is required for p53 stabilization and Ser-15 phosphorylation after IR, as cells from AT patients have significantly reduced p53 protein levels and Ser-15 phosphorylation as compared to normal cells after IR (Siliciano *et al.*, 1997; Shieh *et al.*, 1997; Canman *et al.*, 1998; Banin *et al.*, 1998). To determine if ATM plays a role in MTI-induced elevation of Ser-15 phosphorylation, ATM-deficient fibroblasts (AT-1) were treated with Taxol or nocodazole and the relative levels of Ser-15 phosphorylated p53 determined by Western. MTI treatment did not increase Ser-15 phosphorylation of p53 in the AT-1 fibroblasts after adjustment for the increase in total p53 protein (Figure 3a). However, p53 was not significantly phosphorylated on Ser-15 after MTI treatment in normal human dermal fibroblasts (NHDFs) (Figure 3b), suggesting MTIs induce distinct signaling pathways in fibroblasts that do not increase Ser-15 phosphorylation. Of note, the MTI-mediated increases in total p53 were not significantly reduced in AT-1 cells as compared to the fold increases observed in NHDFs, suggesting that MTI-induced stabilization of p53 is not ATM-dependent (Figure 3). Further, similar p53 phospho-forms were observed in lysates prepared from Taxol-treated NHDF and AT-1 fibroblasts (data not shown).

NHDFs and AT-1 cells were also treated with IR and ADR to verify that Ser-15 phosphorylation of p53 could occur in NHDFs (Figure 3). IR and ADR treatments increased Ser-15 phosphorylated p53 in both NHDFs and AT-1 cells; however, the IR and ADR-induced elevations in total p53 protein levels and Ser-15 phosphorylated p53 were greater in NHDFs as compared to AT-1 fibroblasts (Figure 3).

Analysis of p53 amino terminus phospho-mutant proteins after treatment of cells with MTIs, IR, and ADR

To further investigate p53 phosphorylation after microtubule disruption, p53-deficient H1299 cells were transfected with a panel of expression vectors encoding phosphorylation-site mutant p53 proteins, the cells were treated with Taxol or nocodazole, and the ectopically expressed p53 proteins were examined by 2D gel electrophoresis. The proteins analysed in this study include the following point mutants in which serine or threonine were mutated to alanine: Ser-15 (S15A), Thr-18 (T18A), Ser-20 (S20A), Ser-37 (S37A) (Ashcroft *et al.*, 1999). A Thr-18 point mutant in which threonine was mutated to aspartic acid (T18D) (Ashcroft *et al.*, 1999) and a double mutant in which Ser-15 and Thr-18 (S15A/T18A) (Blattner *et al.*, 1999) were altered to alanine were also used in these experiments. In addition, a p53 mutant (N/C-Term) in which a majority of the previously described p53 amino terminal and carboxy terminal phosphorylation sites were mutated to alanine was examined; this protein contained alanine substitutions at residues 6, 9, 15, 18, 20, 33, 37, 315, 371, 376, 378 and 392 (Ashcroft *et al.*, 1999). Expression of each p53 mutant protein was verified by Western (data not shown).

To determine if ectopically expressed wt p53 was phosphorylated after Taxol treatment, wt p53 was transiently expressed in H1299 cells in the presence or absence of Taxol and evaluated by 2D analysis. A similar number of wt p53 phospho-forms were observed in Taxol-treated H1299 cells as compared to endogenous p53 in Taxol-treated HCT116 cells (Figures 1a and 4a). Further, p53 protein isolated from Taxol-treated H1299 cells had significantly more phospho-forms than the untreated wt p53 control, verifying that ectopically expressed p53 was phosphorylated after MTI treatment (Figure 4a). Alignment by the internal standard protein allowed assignment of P_1, P_2, and P_3 for the ectopically expressed p53 proteins (Figure 4a, S). Initial 2D analysis of each mutant protein was performed in the absence of cellular stress. All the mutants, with the exception of T18D, had a reduced number of p53 phospho-forms as compared to wt p53 (Figure 4b). A significant fraction of the T18A mutant protein was present as the P_1 phospho-form as compared to wt p53 or any other point mutant (Figure 4b). In addition, the N/C-Term p53 mutant migrated at predominantly the P_0 form, a finding consistent with the removal of the majority of

Figure 2 Increased phosphorylation of p53 on Ser-15 in tumor cells after MTI treatment. Western analysis of MDM2, total p53 (PAb1801), Ser-15 phosphorylated p53 (α-Ser-15), p21, and actin protein levels in HCT116 (a) or RKO (b) cells after treatment with Taxol (100 nM), nocodazole (83 nM), IR (10 Gy), and ADR (350 nM). The numbers below the total p53 and Ser-15 phosphorylated p53 panels represent fold increase relative to the 0 h timepoint. (c) Northern analysis of MDM2, p21 and GADPH mRNA levels in HCT116 cells after treatment with nocodazole (83 nM) or Taxol (100 nM). The numbers below each panel represent the fold increase relative to the 0 h timepoint. Results are representative of two independent experiments

the previously described p53 phosphorylation sites (Figure 4b).

To determine if mutation of specific phospho-residues affected the MTI-induced phosphorylation of p53, each of the mutant proteins was expressed in H1299 cells, the cells were treated with Taxol or nocodazole for 24 h, and the ectopically expressed p53 proteins were examined by 2D analysis. Taxol treatment did not significantly increase phosphorylation of the N/C-Term mutant, as the majority of the protein remained as the P_0 form, suggesting Taxol-induced phosphorylation was dependent on the mutated p53 phospho-residues (Figure 5a). All of the amino terminal point mutants examined had reduced p53 phosphorylation as compared to wt p53 after Taxol treatment (Figure 5a). For example, Taxol

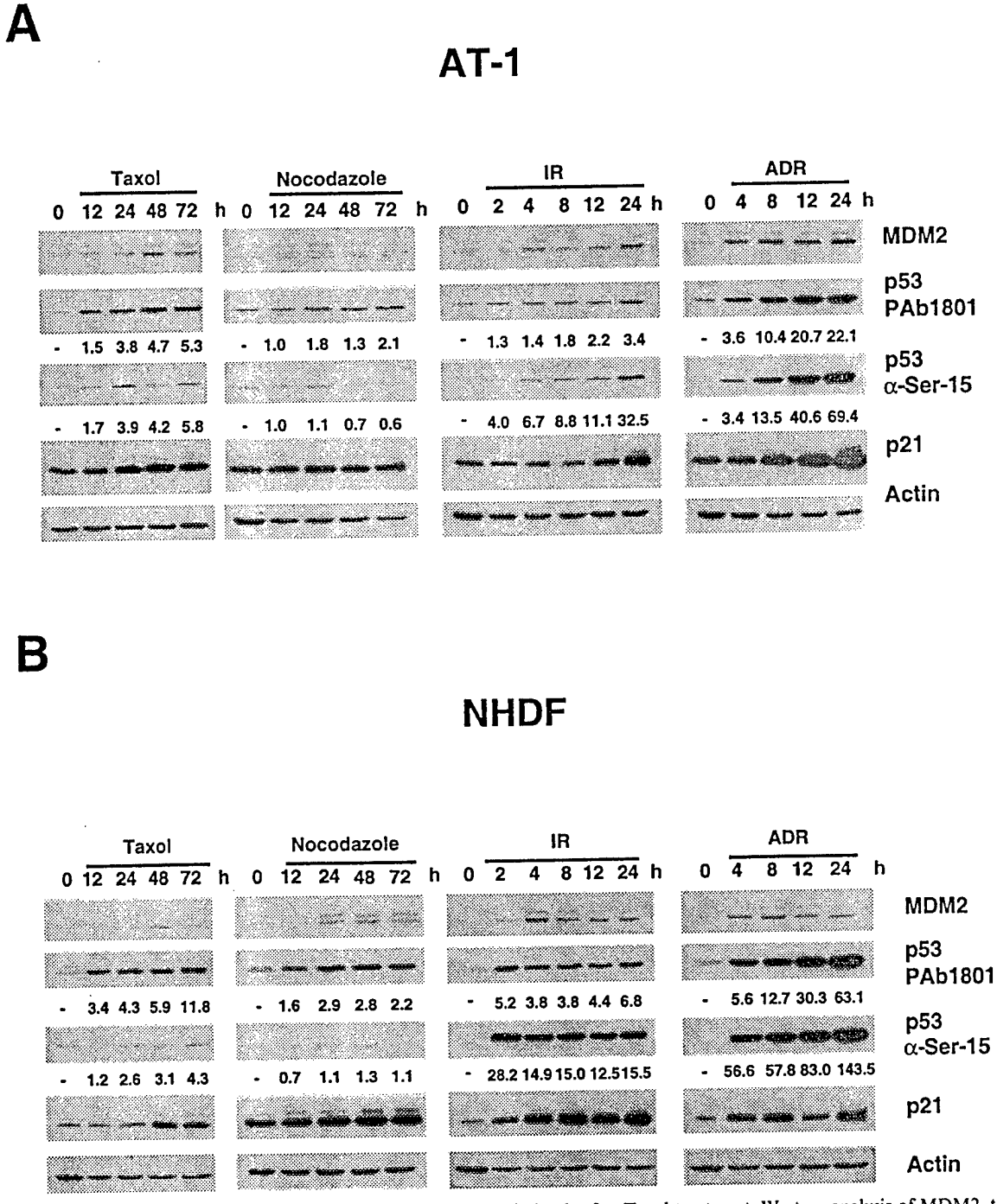

Figure 3 ATM-deficient cells have a delayed increase in p53 protein levels after Taxol treatment. Western analysis of MDM2, total p53 (PAb1801), Ser-15 phosphorylated p53 (α-Ser-15), p21, and actin protein levels in AT-1 (a) or NHDF (b) cells after treatment with Taxol (100 nM), nocodazole (83 nM), IR (10 Gy), and ADR (350 nM). Results are representative of three independent experiments

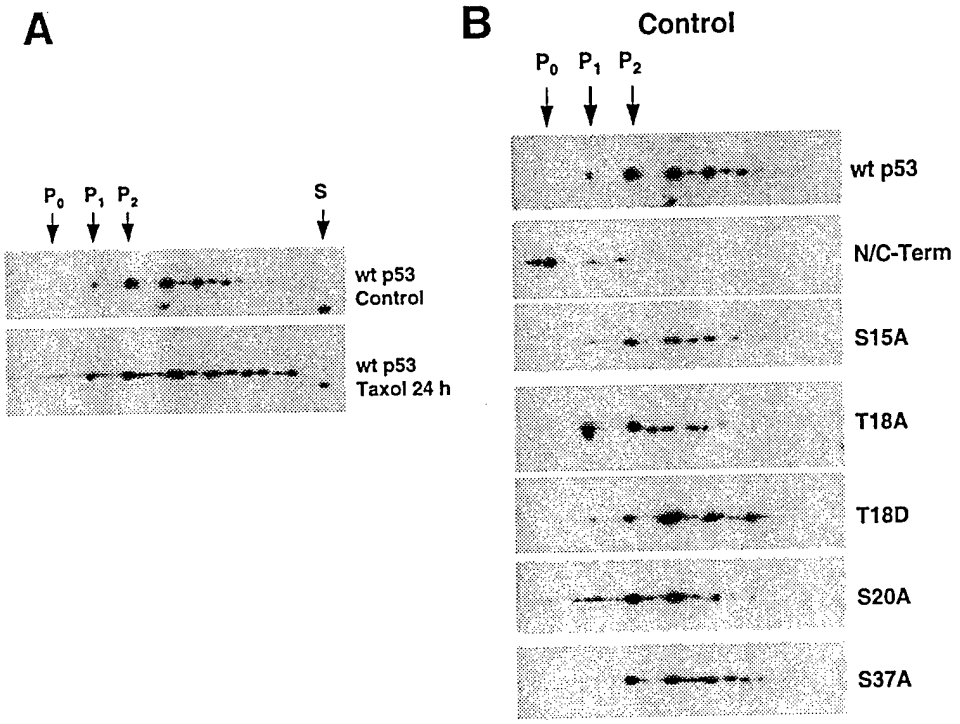

Figure 4 Taxol treatment induces phosphorylation of ectopically expressed p53 on multiple sites. (a) Lysates from control and Taxol-treated (100 nM) H1299 cells transfected with wt p53 were analysed by 2D gel electrophoresis. The P_0 and the P_1 and P_2 phospho-forms in the ectopically expressed p53 proteins were assigned by alignment with the internal standard protein (S). (b) Lysates from untreated H1299 cells transfected with wt p53 or the indicated p53 point mutants were analysed by 2D gel electrophoresis. P_0 and the P_1 and P_2 phospho-forms were assigned by alignment with the internal standard protein. The various p53 phospho-forms (P_0, P_1, P_2) likely comprise a mixture of phosphorylated p53 species with identical mass/charge ratios. Results are representative of three independent experiments

treatment did not increase the number of S15A mutant phospho-forms beyond those observed in the control wt p53. This result was consistent with the detection of Ser-15 phosphorylation in HCT116 and RKO cells after Taxol treatment (Figure 2a,b). The T18A mutant had the most significant reduction in phosphorylation of all the p53 single point mutants evaluated with the majority of the protein in the P_1 form and a lesser amount at P_2 (Figure 5a). Further, replacement of Thr-18 with aspartic acid (T18D) partially rescued p53 phosphorylation (Figure 5a). Taken together, these data suggest that Taxol-induced phosphorylation of p53 requires multiple amino terminal residues that function either as direct phosphorylation sites or as recognition sequences for kinases that phosphorylate other p53 residues.

Similar to Taxol treatment, the nocodazole-treated N/C-Term mutant remained predominantly in the P_1 form (Figure 5b). In contrast to Taxol treatment, mutation of individual p53 amino terminal residues did not significantly impair nocodazole-mediated phosphorylation, suggesting that distinct signaling pathways are activated by these two MTIs (Figure 5b). For example, nocodazole-mediated phosphorylation of the T18A mutant protein resembled that observed with wt p53, with the majority of the protein in the P_2 or greater phosphorylated forms. This result is significantly different from that observed after Taxol treatment, as the majority of the T18A protein was in the P_1 phospho-form after Taxol exposure (Figure 5a,b). Thus, similar to the 2D data obtained with endogenous p53 in HCT116 cells (Figure 1b), analysis of ectopically expressed p53 point mutant proteins suggests that Taxol and nocodazole induce distinct p53 phosphorylation patterns.

Analysis of IR- and ADR-induced phosphorylation of the p53 mutant proteins demonstrated that the S37A mutant had the most significant reduction in p53 phosphorylation as compared to wt p53, suggesting that phosphorylation of Ser-37 is important for subsequent phosphorylation of p53 after genotoxic stress (Figure 5c,d). Like Taxol and nocodazole treatment, IR and ADR treatment did not significantly increase the p53 phospho-forms detected in the N/C-Term mutant (Figure 5c,d). After IR or ADR exposure, the majority of the T18A mutant was present as P_2 or greater phospho-forms (Figure 5c,d), in contrast to Taxol treatment, in which a significant fraction of the T18A mutant protein was present as the P_1 phospho-form (Figure 5a).

To further investigate p53 phosphorylation after MTI treatment, the S15A/T18A double mutant was analysed by 2D electrophoresis. Similar to the untreated T18A mutant, the control S15A/T18A mutant protein had a significantly higher level of the P_1 phospho-form as compared to wt p53 or any other

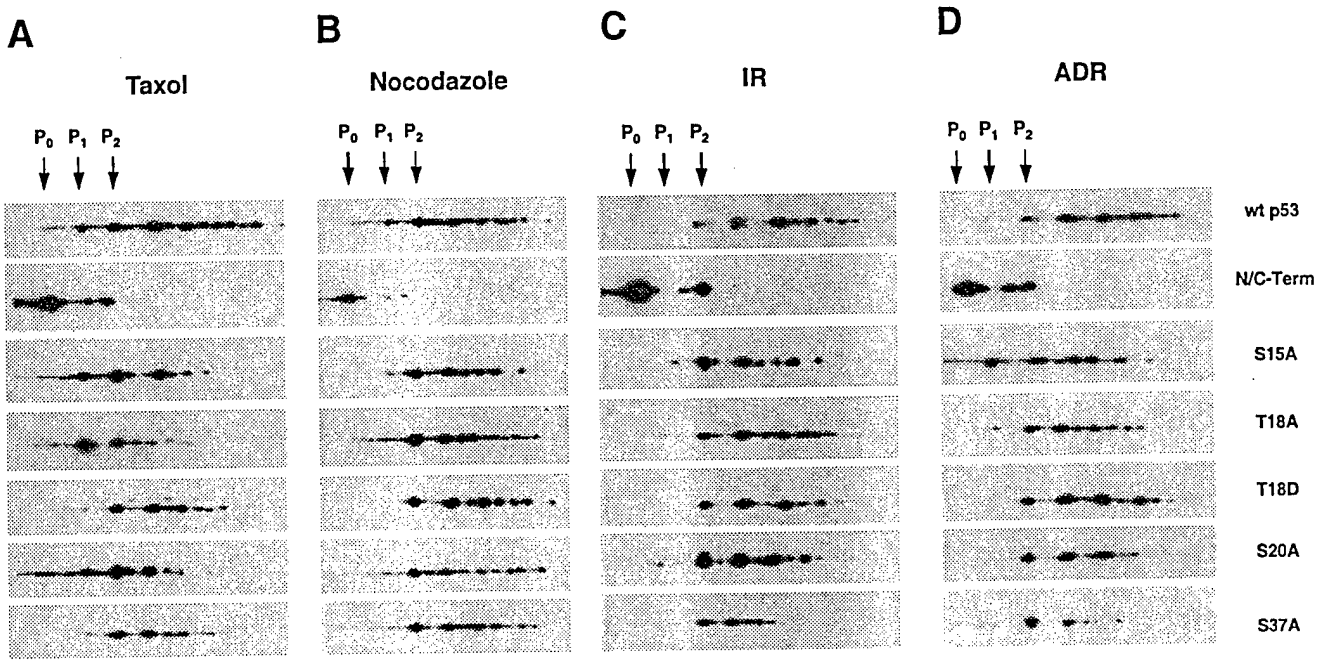

Figure 5 Differential phosphorylation of p53 amino terminal point mutant proteins after MTI, IR, or ADR treatment. Lysates from H1299 cells transfected with wt p53 or the indicated p53 point mutants and treated with (a) Taxol (100 nM), (b) nocodazole (83 nM), (c) IR (10 Gy), or (d) ADR (350 nM) were analysed by 2D gel electrophoresis. P_0 and the P_1 and P_2 phospho-forms were assigned by alignment with the internal standard protein. The various p53 phospho-forms (P_0, P_1, P_2) likely comprise a mixture of phosphorylated p53 species with identical mass/charge ratios. Results are representative of two independent experiments

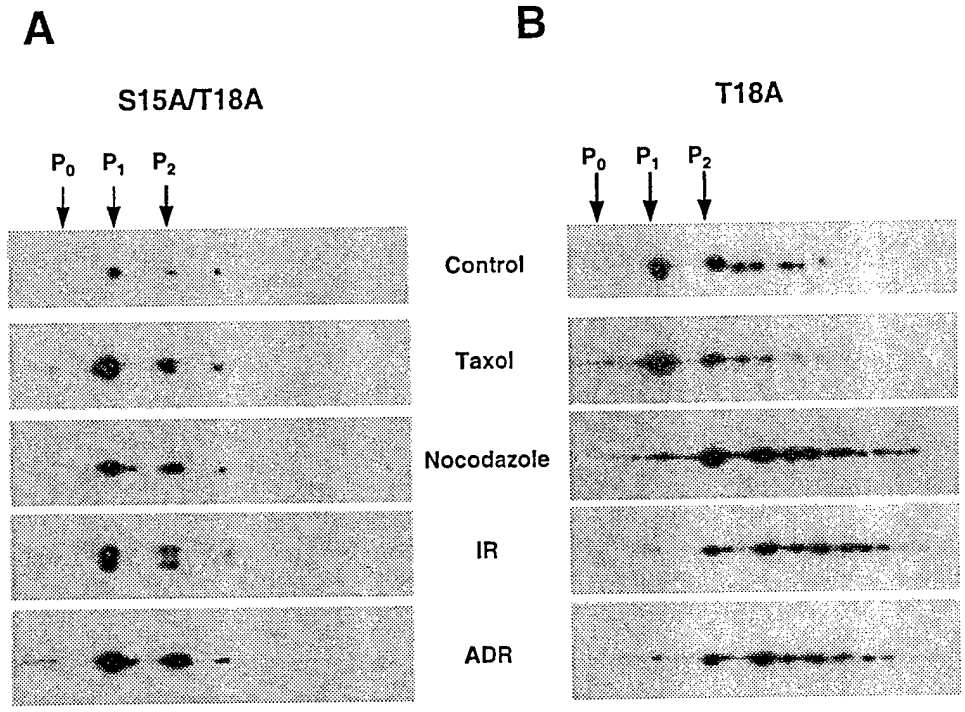

Figure 6 Mutation of Ser-15 and Thr-18 results in reduced phosphorylation of p53 after treatment with MTIs and genotoxic agents. Lysates from H1299 cells transfected with either the S15A/T18A p53 double point mutant (a) or the T18A p53 point mutant (b) and treated with Taxol (100 nM), nocodazole (83 nM), IR (10 Gy), and ADR (350 nM) were analysed by 2D gel electrophoresis. The various p53 phospho-forms (P_0, P_1, P_2) likely comprise a mixture of phosphorylated p53 species with identical mass/charge ratios. Results are representative of two independent experiments

individual point mutant protein (Figures 4b and 6a). In contrast to the single point mutant proteins evaluated, the S15A/T18A mutant protein had a significant reduction in phosphorylation after treatment with either MTIs or genotoxic agents, as the majority of the protein migrated as the P_1 and P_2 phospho-forms (Figure 6a). This finding differs from the phosphorylation patterns observed with either the S15A or T18A point mutant proteins. For example, the S15A mutant protein had reduced phosphorylation after Taxol, nocodazole, IR and ADR treatment as compared to wt p53, but all treatments induced phosphorylation beyond the P_2 phospho-form (Figure 5). Similarly, while the T18A mutant protein had a reduction in phospho-forms after Taxol treatment, it was phosphorylated beyond the P_2 phospho-form after nocodazole, IR, or ADR treatment (Figure 6b). These results suggest that under all conditions examined, phosphorylation of Ser-15 or Thr-18 is required for phosphorylation of subsequent sites.

Discussion

Recent studies have identified signaling pathways that regulate p53 activation after DNA damage or oncogene activation; however, the mechanism(s) by which p53 is activated after microtubule disruption has not been elucidated. The goal of the current study was to analyse p53 phosphorylation after microtubule disruption and to identify specific p53 residues necessary for MTI-induced phosphorylation. Two dimensional gel electrophoresis of p53 from MTI-treated HCT116 cells demonstrated that p53 phosphorylation increased after microtubule disruption and that Vincristine and Taxol induced significantly more phospho-forms than nocodazole. Further, mutation of p53 amino terminal phosphorylation sites significantly impaired Taxol-induced phosphorylation of p53, while nocodazole-mediated phosphorylation was minimally reduced. These data suggest that different upstream signaling pathways are activated by specific MTIs and result in distinct phosphorylation patterns of p53. Further, 2D analysis of ectopically expressed p53 phospho-mutant proteins demonstrated that Thr-18 is a critical residue for subsequent phosphorylation of p53 after Taxol treatment, while Ser-37 is an important residue for subsequent p53 phosphorylation after genotoxic stress. It remains to be determined if Thr-18 and Ser-37 function as direct phosphorylation sites or as part of recognition sequences for kinases that phosphorylate other p53 residues.

In HCT116 and RKO cells, MDM2 mRNA and protein levels increased after nocodazole treatment, whereas after Taxol treatment, MDM2 protein levels decreased, despite an increase in MDM2 mRNA levels. In contrast, both MTIs induced an elevation in p21 mRNA and protein levels. Several groups have reported differential upregulation of p21 and MDM2 after p53 activation; however, there has been concordant regulation of the target gene mRNA and protein levels. For example, camptothecin induced p53-mediated elevation in p21 mRNA and protein levels and failed to increase MDM2 mRNA or protein levels (Ashcroft *et al.*, 2000). Similarly, after exposure to high dose UV, p21 mRNA and protein levels rapidly increased, while MDM2 mRNA and protein levels decreased (Wu and Levine, 1997). Thus, the protein levels of p21 and MDM2 after specific stresses is typically modulated by p53 transcriptional regulation of the respective promoters. The finding that Taxol treatment induces transcriptional upregulation of MDM2 but not an elevation in steady state MDM2 protein levels, suggests the presence of an alternative mechanism that decreases MDM2 protein levels without affecting p53 protein levels.

Several significant findings in this study resulted from experiments using the Ser-15 p53 phospho-specific antibody. For example, in contrast to the elevation in Ser-15 phosphorylated p53 observed in MTI-treated HCT116 and RKO epithelial tumor cells, the elevation in Ser-15 phosphorylated p53 in Taxol-treated NHDFs and ATM-deficient fibroblasts was only reflective of the increase in total p53 protein. These results suggest that the non-transformed fibroblasts and transformed epithelial tumor cells examined in this study induce distinct signaling pathways after microtubule disruption, resulting in differential phosphorylation of p53.

Adding a further layer of complexity to interpretation of the biological consequences of p53 phosphorylation are recent studies indicating that there is interplay between the phospho-sites, such that phosphorylation on one residue may require phosphorylation on a prior site. For example, Bulavin *et al.* (1999) observed that substitution of alanine at Ser-33 completely blocked UV-induced phosphorylation at Ser-37 but did not decrease phosphorylation at Ser-15. In contrast, the S33A/S46A double mutant abrogated UV-induced phosphorylation of Ser-37, and significantly reduced phosphorylation at Ser-15 (Bulavin *et al.*, 1999). This previous finding suggests that either the presence of Ser-33 and Ser-46 residues, or their ability to be phosphorylated, is important for amino terminal phosphorylation of p53 after cells are exposed to UV light. Similarly, Sakaguchi *et al.* (2000) and Dumaz *et al.* (1999) recently reported that IR-induced phosphorylation of p53 on Thr-18 required prior phosphorylation on Ser-15. The results from the current study are consistent with these latter studies, as the S15A/T18A double mutant was not significantly phosphorylated after microtubule disruption or genotoxic stress, in contrast to the T18A single point mutant protein that was phosphorylated after nocodazole, IR and ADR treatments.

Currently, a major challenge in the p53 field is linking biochemical modifications of the protein with biological effects. The studies cited above and the results presented in the current study illustrate the need for higher resolution techniques that will allow analysis of p53 after cellular stress. Mass spectrometric analysis of the p53 protein was recently used by Abraham *et al.* (2000) to identify p53 sites that are covalently modified

in vivo, either constitutively or in response to IR. By identifying specific post-translational modifications after cellular stress, the biochemical activity of differentially modified p53 molecules at specific promoters can begin to be evaluated. For example, co-analysis of p53 by mass spectroscopy and *in vivo* promoter-trapping (Murphy *et al.*, 1999; Szak and Pietenpol, (2000)) after a specific cellular stress may allow important insight to the p53 post-translational modifications required for a biological endpoint.

Since drugs that alter microtubule dynamics such as Taxol are important anticancer agents, identifying the post-translational modifications that mediate elevation of p53 protein levels after microtubule disruption in tumor cells may have important therapeutic implications. The results from this study indicate that MTI treatment of epithelial tumor cells results in distinct patterns of phosphorylation as compared to genotoxic stress. However, we cannot rule out that microtubule disruption leads to DNA alterations in cells. Thus, the p53 phospho-forms observed may be due to DNA damage signaling pathways distinct from those induced by the genotoxic agents examined in this study. The elucidation of kinases that regulate phosphorylation of p53 after MTI treatment may ultimately identify novel targets for chemotherapeutic intervention. For example, loss of p53 function in tumor cells can enhance cellular sensitivity to MTIs (Stewart *et al.*, 1999b). Thus, the development of compounds which inhibit kinases that phosphorylate and activate p53 after microtubule disruption may enhance therapeutic efficacy when these compounds are combined with MTIs to treat tumors with intact p53 signaling pathways.

Materials and methods

Cell culture and treatment

The HCT116 and RKO human colorectal carcinoma cell lines were obtained from American Type Culture Collection (ATCC) and were maintained in monolayer culture in McCoys 5A modified medium (Gibco–BRL) supplemented with 10% fetal bovine serum (FBS; Gemini Bio-Products, Inc.), and 1% penicillin/streptomycin (Sigma). H1299 human large cell lung carcinoma cells (ATCC) have a partial homozygous deletion of the p53 gene, and p53 protein expression is not detectable (Mitsudomi *et al.*, 1992). H1299 cells were maintained in monolayer culture in F-12 medium (Sigma) supplemented with 10% FBS and 1% penicillin/streptomycin. Normal human dermal fibroblasts (NHDFs) (Vanderbilt University Research Center) were maintained in monolayer culture in Dulbecco's Modified Eagle Medium-Hi Glucose (Gibco–BRL) supplemented with 10% FBS and 1% penicillin/streptomycin. The GM02052C (AT-1) fibroblast cell line derived from AT patients (Coriell Institute for Medical Research) was maintained in monolayer culture in Minimum Essential Medium with Earle's salts (Hyclone) supplemented with 15% FBS, 1% penicillin/streptomycin, 2 mM non-essential amino acids (Hyclone), 50 μg/ml insulin-transferrin-selenium A (Boehringer Mannheim), 1 mM MEM amino acids (Gibco–BRL), and MEM vitamins (Gibco–BRL). All cells were grown at 37°C with 5% CO_2 in a humidified incubator.

When indicated, cells were treated with nocodazole (Sigma), paclitaxel (Taxol; Sigma), or Vincristine (Eli Lilly and Co.) diluted in dimethyl sulfoxide and added directly to cell media. Cells were also treated with adriamycin (ADR) (Gensia Sicor Inc.) diluted in media, ionizing radiation (IR), or ultraviolet radiation (UV) when indicated. IR was delivered at room temperature with a ^{137}Cs irradiator (JL Shepherd and Associates). UV was delivered at room temperature with a UV Stratalinker (Stratagene Cloning Systems).

Western analysis

Cell lysates were prepared and transferred onto membranes as previously described (Stewart *et al.*, 1999a). Membranes were incubated with mouse monoclonal antibodies against p53 (PAb1801), p21 (EA10) (Oncogene Research Products), and MDM2 (SMP14) (Santa Cruz Biotechnology); a rabbit polyclonal antibody against serine-15 phosphorylated p53 (New England Biolabs); and a goat polyclonal antibody against actin (I-19) (Santa Cruz Biotechnology). Primary antibodies were detected using goat α-mouse, goat α-rabbit, or rabbit α-goat horseradish peroxidase-conjugated secondary antibodies (Pierce) and enhanced chemiluminescence detection.

Northern analysis

mRNA was isolated from control and MTI-treated HCT116 cells, resolved by agarose gel electrophoresis, and transferred to nitrocellulose membrane (Gibco–BRL) as previously described (Flatt *et al.*, 2000). Human MDM2, p21, and GADPH cDNAs were labeled with α-^{32}P-dCTP using Rediprime II (Amersham). After a 2 h prehybridization incubation in Express Hyb (Clontech Laboratories, Inc.) at 50°C, membranes were incubated with 1×10^6 c.p.m. of labeled cDNA per ml in Express Hyb at 50°C overnight. Membranes were washed twice in 2×SSC and 0.1% SDS (1×SSC is 0.15 M NaCl plus 0.015 M sodium citrate) at 50°C, followed by two washes in 0.2×SSC and 0.1% SDS at 50°C. The hybridized ^{32}P-labeled cDNAs were used to quantify mRNA levels on an Instant Imager (Packard Instrument) prior to autoradiography.

Two dimensional gel electrophoresis

For two dimensional (2D) gel analyses of endogenous p53 in HCT116 cells, 1 mg of protein lysate from control cells or 150 μg of protein lysate from treated cells were prepared in a final volume of 600 μl of isoelectric focusing (IEF) sample buffer (9.5 M urea (Pharmacia), 2% NP-40, 2% β-mercaptoethanol, 0.2% ampholytes pH 5-8 (Pharmacia), 0.001% bromophenol blue). For 2D analyses of p53 ectopically expressed in H1299 cells, 75 μg of protein lysate were prepared in a final volume of 600 μl of IEF sample buffer. A truncated form of recombinant human p53 (amino acids 1–353) was incubated in each sample as an internal standard to permit alignment of p53 phospho-forms; the truncated human p53 was prepared as previously described (Szak and Pietenpol, 1999). IEF was performed using the PROTEAN IEF system (Biorad) and 17 cm isoelectric strip gels pH 5-8 (Biorad). The isoelectric gels were passively rehydrated for 6 h in IEF sample buffer containing the protein lysate prior to focusing for 60 000 volt-hours. After IEF, gels were incubated for 15 min in equilibration buffer I (6M urea, 2% SDS, 0.375 M Tris (pH 8.8), 20% glycerol, 130 mM DTT) and 15 min in equilibration buffer II (6M urea, 2% SDS, 0.375 M Tris (pH 8.8), 20% glycerol, 135 mM iodoacetamide

(Aldrich Chemical Company, Inc.)) prior to separation by SDS–PAGE.

Potato acid phosphatase treatment of protein lysates

HCT116 protein lysates (150 μg) were incubated in 40 mM PIPES pH 6.0 (final volume 100 μl) for 10 min at 30°C, followed by addition of 2.0 units of potato acid phosphatases (Boehringer Mannheim). The incubation was continued for 30 min at 30°C. As a control for non-specific proteolytic degradation, protein lysates were also incubated in the absence of phosphatase under the same conditions. Phosphatase reactions were stopped by addition of Laemmli SDS–PAGE or IEF sample buffer.

Expression of p53 phosphorylation-site mutants

A panel of p53 phosphorylation-site mutants containing either alanine or aspartic acid substitutions for the indicated residues and the pCB6+ parental vector were a generous gift from Karen Vousden (National Cancer Institute, Frederick, MD, U.S.A.) (Ashcroft *et al.*, 1999). The p53 mutants include: serine-15 (S15A), threonine-18 (T18A and T18D), serine-20 (S20A), serine-37 (S37A), and a combination mutant with N-terminal and C-terminal phosphorylation sites modified to alanine (S6A, S9A, S15A, T18A, S20A, S33A, S37A, S315A, S371A, S376A, S378A, S392A). The double p53 phosphorylation-site mutant S15A/T18A in the retroviral vector pLXSN was a generous gift of Peter Herrlich (Institut für Genetik, Karlsruhe, Germany) (Blattner *et al.*, 1999). The cDNAs encoding wt p53 (*Kpn*I–*Bam*HI fragment) and the S15A/T18A mutant protein (*Eco*RI fragment) were subcloned into the pCB6+ vector. All expression vectors were verified by sequencing.

Acknowledgments
The authors thank Drs Karen Vousden (NCI) and Peter Herrlich (Institut für Genetik) for the p53 phosphorylation-site mutants. This work was supported by Susan G. Komen Breast Cancer Foundation Grant 99-3038 (ZA Stewart), National Institutes of Health Institutional Training Grant GM07347 (ZA Stewart), National Institutes of Health Grant CA70856 (JA Pietenpol), US Army Grant DAMD17-99-1-9422 (JA Pietenpol), and National Institutes of Health Grants ES00267 and CA68485 (Core services).

References

Abraham J, Kelly J, Thibault P and Benchimol S. (2000). *J. Mol. Biol.*, **295**, 853–864.
Ashcroft M, Kubbutat MHG and Vousden KH. (1999). *Mol. Cell. Biol.*, **19**, 1751–1758.
Ashcroft M, Taya Y and Vousden KH. (2000). *Mol. Cell. Biol.*, **20**, 3224–3233.
Banin S, Moyal L, Shieh SY, Taya Y, Anderson CW, Chessa L, Smorodinsky NI, Prives C, Reiss Y, Shiloh Y and Ziv Y. (1998). *Science*, **281**, 1674–1677.
Baudier J, Delphin C, Grunwald D, Khochbin S and Lawrence JJ. (1992). *Proc. Natl. Acad. Sci. USA*, **89**, 11627–11631.
Blattner C, Tobiasch E, Litfen M, Rahmsdorf HJ and Herrlich P. (1999). *Oncogene*, **18**, 1723–1732.
Bulavin DV, Saito S, Hollander MC, Sakaguchi K, Anderson CW, Appella E and Fornace Jr AJ. (1999). *EMBO J.*, **18**, 6845–6854.
Canman CE and Lim DS. (1998). *Oncogene*, **17**, 3301–3308.
Canman CE, Lim DS, Cimprich KA, Taya K, Tamai K, Sakaguchi K, Appella E, Kastan MB and Siliciano JD. (1998). *Science*, **281**, 1677–1679.
Chehab NH, Malikzay A, Stavridi ES and Halazonetis TD. (1999). *Proc. Natl. Acad. Sci. USA*, **96**, 13777–13782.
Chehab NH, Malikzay A, Appel M and Halazonetis TD. (2000). *Genes Dev.*, **14**, 278–288.
Craig AL, Burch L, Vojtesek B, Mikutowska J, Thompson A and Hupp TR. (1999). *Biochem. J.*, **342**, 133–141.
Cross SM, Sanchez CA, Morgan CA, Schimke MK, Ramel S, Idzerda RL, Raskind WH and Reid BJ. (1995). *Science*, **267**, 1353–1356.
Cuddihy AR, Wong AH, Tam NW, Li S and Koromilas AE. (1999). *Oncogene*, **18**, 2690–2702.
Di Leonardo A, Khan SH, Linke SP, Greco V, Seidita G and Wahl GM. (1997). *Cancer Res.*, **57**, 1013–1019.
Dumaz N, Milne DM and Meek DW. (1999). *FEBS Lett.*, **463**, 312–316.
Flatt PM, Tang LJ, Scatena CD, Szak ST and Pietenpol JA. (2000). *Mol. Cell. Biol.*, **20**, 4210–4223.
Furnari B, Rhind N and Russell P. (1997). *Science*, **277**, 1495–1497.
Gao CF, Nakajima T, Taya Y and Tsuchida N. (1999). *Biochem. Biophys. Res. Commun.*, **264**, 860–864.
Hall SR, Campbell LE and Meek DW. (1996). *Nucleic Acids Res.*, **24**, 1119–1126.
Hall-Jackson CA, Cross DA, Morrice N and Smythe C. (1999). *Oncogene*, **18**, 6707–6713.
Haupt Y, Maya R, Kazaz A and Oren M. (1997). *Nature*, **387**, 296–299.
Hecker D, Page G, Lohrum M, Weiland S and Scheidtmann KH. (1996). *Oncogene*, **12**, 953–961.
Hirao A, Kong YY, Matsuoka S, Wakeham A, Ruland J, Yoshida H, Liu D, Elledge SJ and Mak TW. (2000). *Science*, **287**, 1824–1827.
Hupp TR, Meek DW, Midgley CA and Lane DP. (1992). *Cell*, **71**, 875–886.
Khan SH and Wahl GM. (1998). *Cancer Res.*, **58**, 396–401.
Khosravi R, Maya R, Gottlieb T, Oren M, Shiloh Y and Shkedy D. (1999). *Proc. Natl. Acad. Sci. USA*, **96**, 14973–14977.
Knippschild U, Milne DM, Campbell LE, DeMaggio AJ, Christenson E, Hoekstra MF and Meek DW. (1997). *Oncogene*, **15**, 1727–1736.
Kubbutat MHG, Jones SN and Vousden KH (1997). *Nature*, **387**, 299–303.
Lanni JS and Jacks T. (1998). *Mol. Cell. Biol.*, **18**, 1055–1064.
Lavin MF and Shiloh Y. (1996). *Curr. Opin. Immunol.*, **8**, 459–464.
Lees-Miller SP, Sakaguchi K, Ullrich SJ, Appella E and Anderson CW. (1992). *Mol. Cell. Biol.*, **12**, 5041–5049.
Li L, Ljungman M and Dixon JE. (2000). *J. Biol. Chem.*, **275**, 2410–2414.
Matsuoka S, Huang M and Elledge SJ. (1998). *Science*, **282**, 1893–1897.
Mayo LD, Turchi JJ and Berberich SJ. (1997). *Cancer Res.*, **57**, 5013–5016.
Milne DM, Palmer RH, Campbell DG and Meek DW. (1992). *Oncogene*, **7**, 1361–1369.

remove
insert
period

Mitsudomi T, Steinberg SM, Nau MM, Carbone D, D'Amico D, Bodner S, Oie HK, Linnoila RI, Mulshine JL, Minna JD and Gazdar AF. (1992). *Oncogene*, **7**, 171–180.

Murphy M, Ahn J, Walker KK, Hoffman WH, Evans RM, Levine AJ and George DL. (1999). *Genes Dev.*, **13**, 2490–2501.

Sakaguchi K, Saito S, Higashimoto Y, Roy S, Anderson CW and Appella E. (2000). *J. Biol. Chem.*, **275**, 9278–9283.

Sanchez Y, Wong S, Thoma RS, Richman R, Wu Z, Piwnica-Worms H and Elledge SJ. (1997). *Science*, **277**, 1497–1501.

Sherr CJ and Weber JD. (2000). *Curr. Opin. Genet. Dev.*, **10**, 94–99.

Shieh SY, Ikeda M, Taya Y and Prives C. (1997). *Cell*, **91**, 325–334.

Shieh SY, Ahn J, Tamai K, Taya Y and Prives C. (2000). *Genes Dev.*, **14**, 289–300.

Siliciano JD, Canman CE, Taya Y, Sakaguchi K, Appella E and Kastan MB. (1997). *Genes Dev.*, **11**, 3471–3481.

Stewart ZA, Leach SD and Pietenpol JA. (1999a). *Mol. Cell Biol.*, **19**, 205–215.

Stewart ZA, Mays D and Pietenpol JA. (1999b). *Cancer Res.*, **59**, 3831–3837.

Szak ST and Pietenpol JA. (1999). *J. Biol. Chem.*, **274**, 3904–3909.

~~Szak ST and Pietenpol JA. (2000). ???, in press.~~ remove (1)

Tibbetts RS, Brumbaugh KM, Williams JM, Sarkaria JN, Cliby WA, Shieh SY, Taya Y, Prives C and Abraham RT. (1999). *Genes Dev.*, **13**, 152–157.

Wang Y and Prives C. (1995). *Nature*, **376**, 88–91.

Waterman MJF, Stavridi ES, Waterman JLF and Halazonetis TD. (1998). *Nature Genet.*, **19**, 175–178.

Wu L and Levine AJ. (1997). *Mol. Med.*, **3**, 441–451.